Universität Zürich[UZH]

Limits on total lepton number and lepton flavour asymmetries from BBN and the CMB

PASCOS 2026,
25th June 2026,
Sheffield, UK

Mario Fernández Navarro

Based on:

Valerie Domcke, Miguel Escudero, MFN, Stefan Sandner, JHEP 06 (2025) 137, [2502.14960]

Valerie Domcke, Miguel Escudero, MFN, Stefan Sandner, JCAP 02 (2026) 017, [2510.02438]

This talk

1. A fast and reliable formalism to evolve lepton flavour asymmetries from the onset of neutrino oscillations to BBN times

2. Constraints on flavour directions for the total lepton number conserving scenario $L \approx 0$

3. A bound on the total lepton number of the Universe from BBN and the CMB

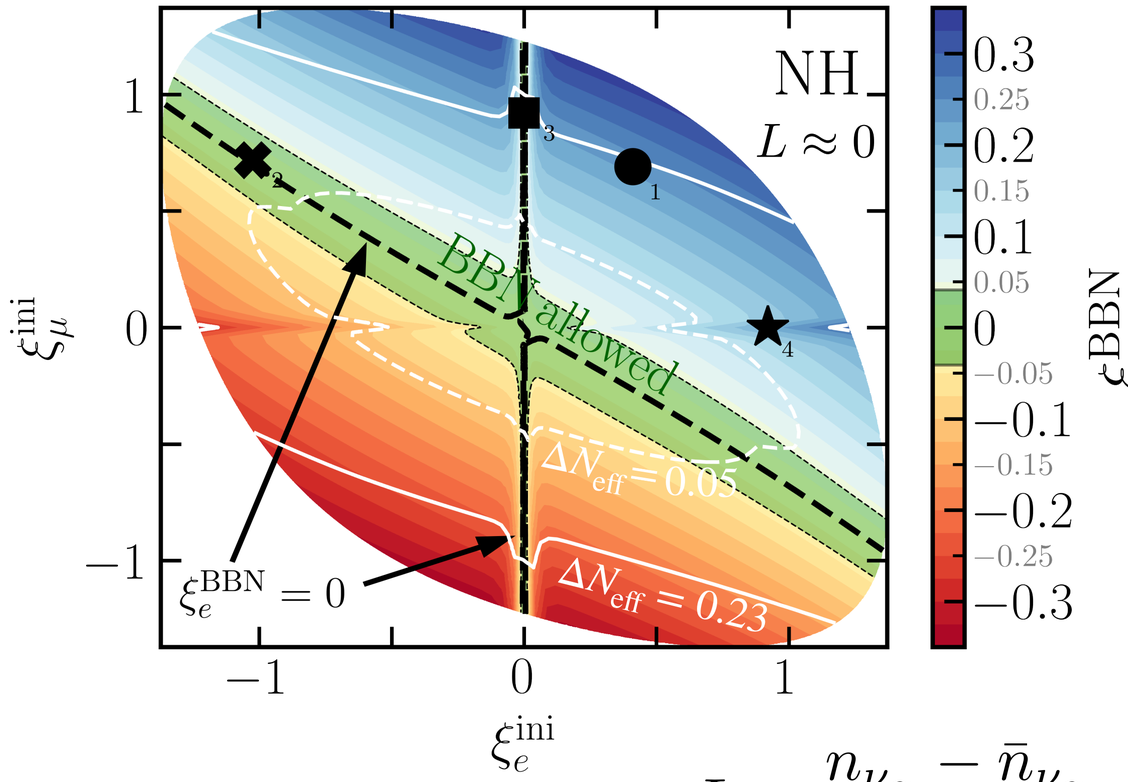

$$L = \frac{n_{\nu_\alpha} - \bar{n}_{\nu_\alpha}}{T^3}$$

$$(\xi_e, \xi_\mu, \xi_\tau) \rightarrow \texttt{COFLASY} \rightarrow (\xi_e^{\rm BBN}, \Delta N_{\rm eff}, Y_p)$$

$$-0.10(0.08) \leq L \leq 0.10(0.08)$$

NH(IH)

Why large lepton asymmetries

Leptoflavourgenesis

large compensated flavour asymmetries can source baryogenesis

$$L_\tau \lesssim 10^{-5} \quad L_e = -L_\mu \lesssim 10^{-3}$$

[Mukaida, Schmitz, Yamada, '21]

QCD phase transition

large chemical potentials may make QCD first order

[Gao and Oldengott '21]
[Gao *et al* '24] …

Sterile-neutrino DM

Shi–Fuller production requires a matter asymmetry

See talk by Julien Froustey!

Cosmic neutrino background

asymmetries affect future detection prospects

[Stodolski '75, Duda *et al* '01]

EMPRESS low-Y_P anomaly

low helium can point to $\xi_e^{\rm BBN} \sim 0.05$

[EMPRESS, '26]

- Some generation mechanisms:

Affleck–Dine leptoflavourogenesis

large flavour asymmetries with

$$L_e + L_\mu + L_\tau = 0$$

Q-balls can delay their release

[Akita et al, 25']

Late HNL oscillations

ARS freeze-in leptogenesis can generate late active asymmetries

$$L_{\rm active} \neq 0$$

even after sphaleron freeze-out

The (flavour) asymmetric Universe

- If lepton flavour asymmetries survive until neutrino decoupling and BBN times ($T \lesssim 1$ MeV), then they affect the neutron to proton ratio and $N_{\rm eff}$

- Assuming thermal equilibrium:

$$\begin{aligned} p + e^- &\rightleftarrows n + \nu_e \\ p + \overline{\nu}_e &\rightleftarrows n + e^+ \end{aligned} \longrightarrow \frac{n_n}{n_p} \approx \left.\frac{n_n}{p_n}\right|_{\xi_e=0} e^{-\xi_e}$$

$$N_{\rm eff} = \frac{8}{7}\left(\frac{11}{4}\right)^{4/3}\frac{\rho_\nu}{\rho_\gamma} \qquad \Delta N_{\rm eff} = N_{\rm eff} - N_{\rm eff}^{\rm SM} = \sum_\alpha \frac{30}{7}\left(\frac{\xi_\alpha}{\pi}\right)^2 + \frac{15}{7}\left(\frac{\xi_\alpha}{\pi}\right)^4$$

- This translates into the 95% CL bounds:

$$\xi \equiv \frac{\mu}{T}$$

$$\left|\xi_e\right|_{T=T_{\rm BBN}} \lesssim 0.03 \qquad \Delta N_{\rm eff} \lesssim 0.23$$

[Pitrou *et al* '18 …] [Planck '18]

The (flavour) asymmetric Universe

- If le
- ther
- Assu
- $N_{\rm ef}$
- Thi

- But at 20 MeV neutrino oscillations become effective and may lead to flavour equilibration, such that at BBN times $\xi_\alpha \approx 0$ if $L \approx 0$.

$$\Delta n_\alpha = \frac{(n-\bar{n})_{\alpha\alpha}}{T^3}$$

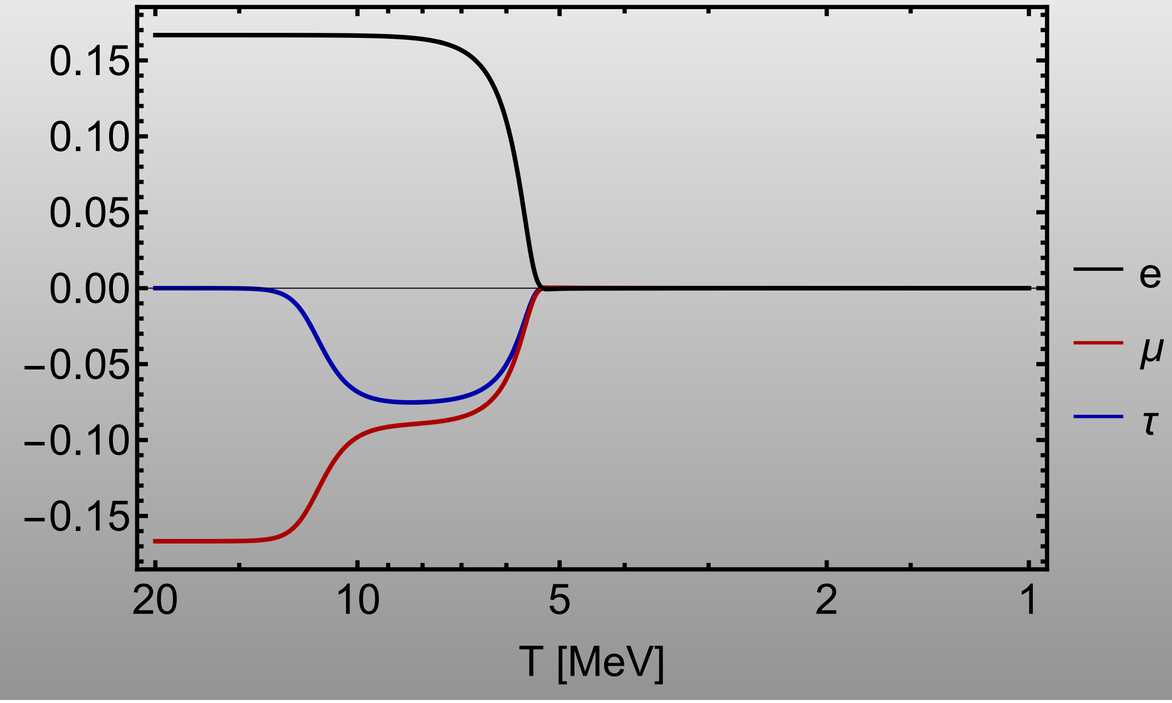

$$\Delta n^{\rm final} \approx \frac{\Delta n_e^{\rm ini} + \Delta n_\mu^{\rm ini} + \Delta n_\tau^{\rm ini}}{3} \approx 0$$

$$\left.\right)^4$$

$$\xi \equiv \frac{\mu}{T}$$

$$|\xi_e|_{T=T_{\rm BBN}} \lesssim 0.03 \qquad \Delta N_{\rm eff} \lesssim 0.23$$

[Pitrou *et al* '18 …] [Planck '18]

The (flavour) asymmetric Universe

- If le
- ther
- Assu
- $N_{\rm ef}$
- Thi

- However, pioneering work suggested that flavour equilibration may not be perfect, revealing a strong sensitivity to θ_{13} which was poorly measured at the time:

[Dolgov *et al* '02, Pastor *et al* '08, Mangano *et al* '10, Castorina *et al* '12…]

$$\Delta n_\alpha = \frac{(n-\bar{n})_{\alpha\alpha}}{T^3}$$

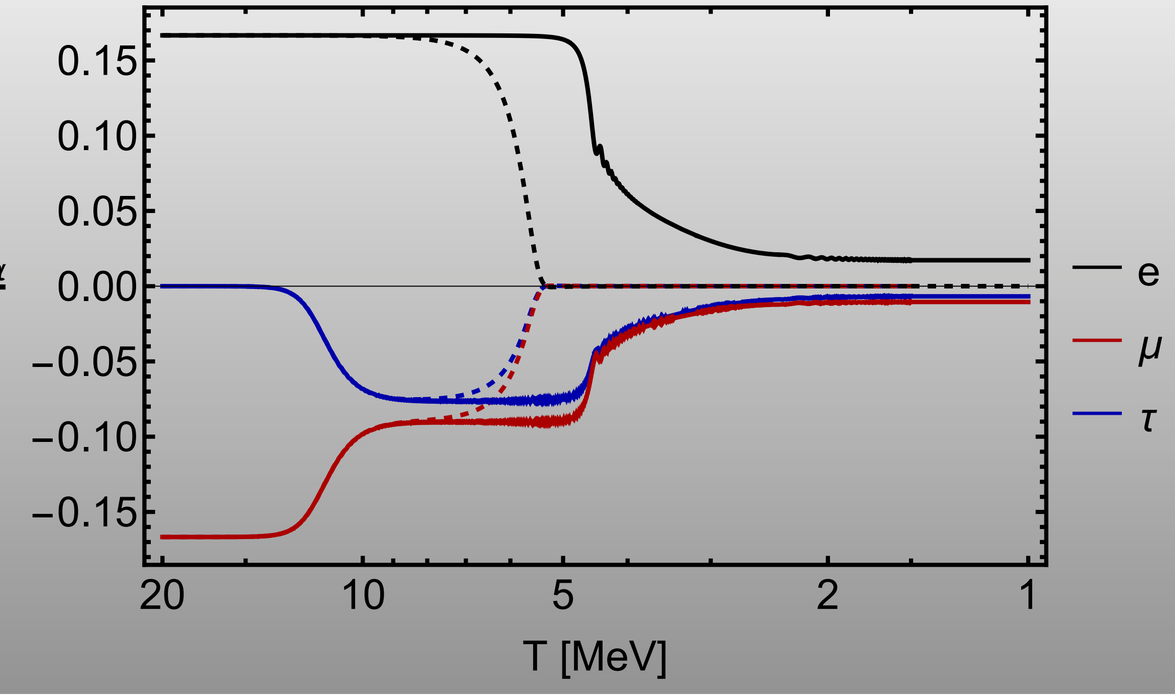

$$\Delta n^{\rm final} \approx \frac{\Delta n_e^{\rm ini} + \Delta n_\mu^{\rm ini} + \Delta n_\tau^{\rm ini}}{3} \approx 0$$

COFLASY-M (Mathematica)

$$|\xi_e|_{T=T_{\rm BBN}} \lesssim 0.03 \qquad \Delta N_{\rm eff} \lesssim 0.23$$

[Pitrou *et al* '18 …] [Planck '18]

The (flavour) asymmetric Universe

- If le… …V),
  ther…
- Assu… $-\xi_e$
- N_{ef} … $\Big)^4$
- Thi…

- Can we actually map the asymmetries at 20 MeV to the asymmetries at 1 MeV and systematically explore the parameter space?

$$\Delta n_\alpha = \frac{(n-\bar{n})_{\alpha\alpha}}{T^3}$$

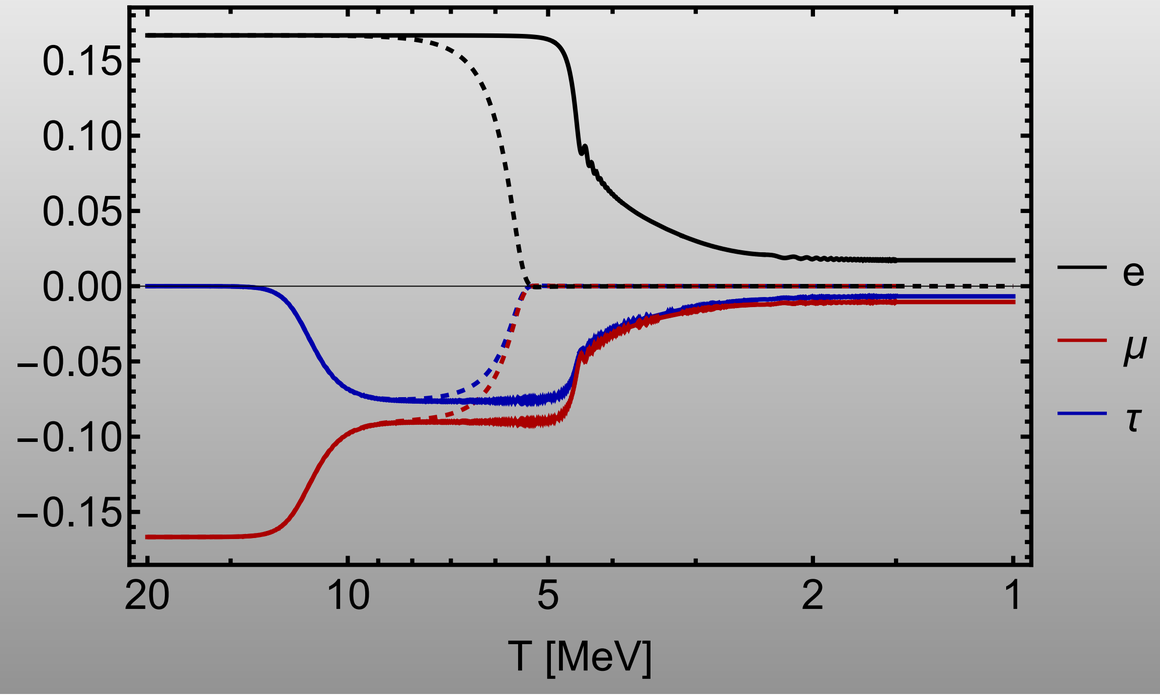

$$\Delta n^{\rm final} \approx \frac{\Delta n_e^{\rm ini} + \Delta n_\mu^{\rm ini} + \Delta n_\tau^{\rm ini}}{3} \approx 0$$

COFLASY-M (Mathematica)

$$\xi \equiv \frac{\mu}{T}$$

$$|\xi_e|_{T=T_{\rm BBN}} \lesssim 0.03 \qquad \Delta N_{\rm eff} \lesssim 0.23$$

[Pitrou *et al* '18 …] [Planck '18]

Quantum Kinetic Equations

$$\frac{d\rho}{dt} = -i\,[\mathcal{H}_0 + V_c + V_s, \rho] + \mathcal{I}(\rho)\,, \qquad \frac{d\overline{\rho}}{dt} = +i\,[\mathcal{H}_0 + V_c - V_s, \overline{\rho}] + \overline{\mathcal{I}}(\overline{\rho})\,,$$

[Sigl and Raffelt '93 …]

$$\rho = \begin{pmatrix} f_{\nu_e} & \rho_{e\mu} & \rho_{e\tau} \\ \rho_{\mu e} & f_{\nu_\mu} & \rho_{\mu\tau} \\ \rho_{\tau e} & \rho_{\tau\mu} & f_{\nu_\tau} \end{pmatrix}$$

- System of integro-differential equations for the neutrino density matrix, including neutrino distribution functions and flavour correlations.
- Need to solve for each momentum mode!

Vaccuum oscillations

$$\mathcal{H}_0 = U_{\rm PMNS}\frac{1}{2k}{\rm diag}(0, \Delta m^2_{21}, \Delta m^2_{31})U^\dagger_{\rm PMNS}$$

Matter potential

$$V_c = -2\sqrt{2}G_F\frac{k}{m_W^2}(\mathbb{E} + \mathbb{P})_{\alpha\alpha}T_\gamma^4$$

Self-interactions (vanishes if no asymmetries)

$$V_s = \sqrt{2}G_F\int\frac{d^3k'}{(2\pi)^3}(\rho - \overline{\rho})$$

Dynamics

- For initial asymmetries relevant for BBN, V_s always dominates and is momentum independent:

→ All momentum modes become aligned and perform synchronous oscillations

[Pastor, Raffelt, Semikoz, '01] …

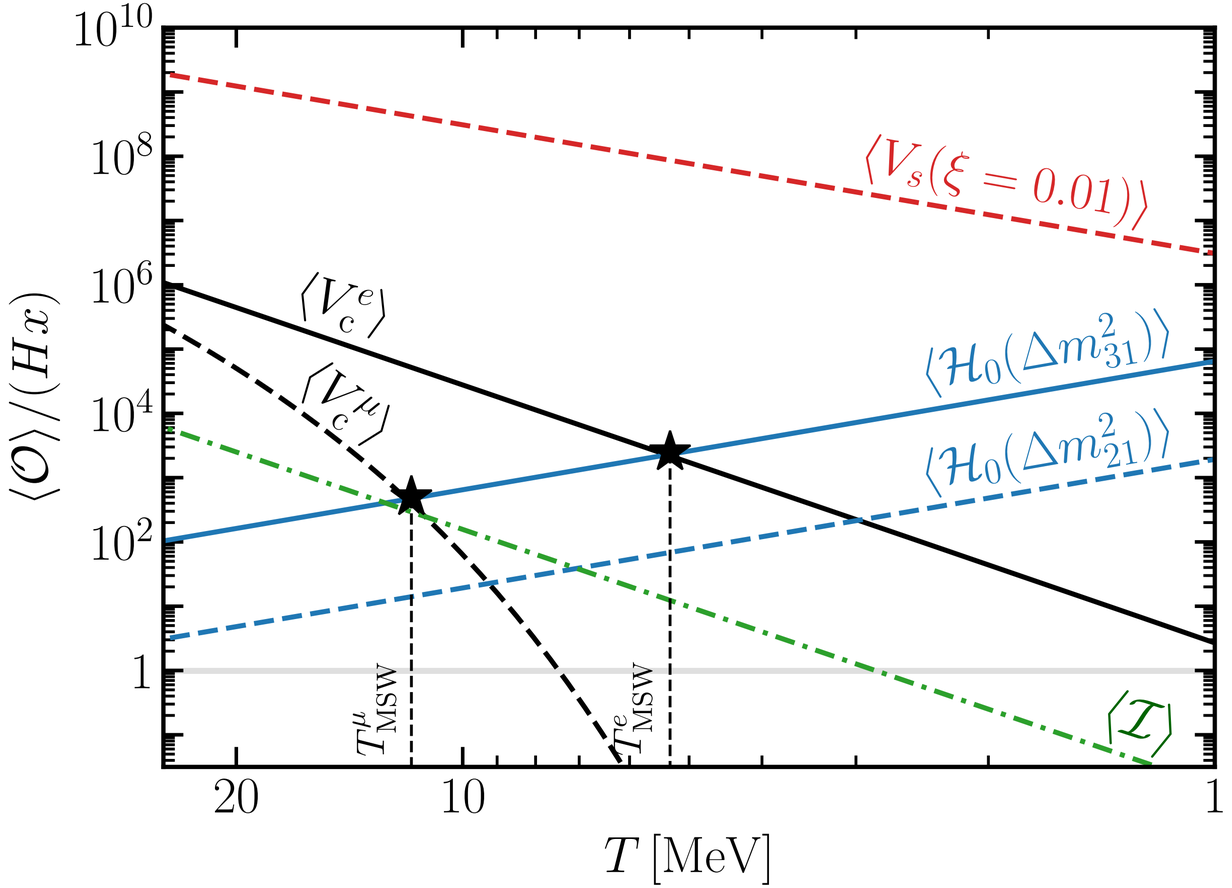

Dynamics

- For initial asymmetries relevant for BBN, V_s always dominates and is momentum independent:

→ All momentum modes become aligned and perform synchronous oscillations

[Pastor, Raffelt, Semikoz, '01] …

- Level crossings from V_c to $\mathscr{H}_0$ lead to muon and electron driven MSW transitions:
  - Muon-driven MSW at $T \approx 12$ MeV
  - Electron-driven MSW at $T \approx 5$ MeV

- At low T, collisions become inefficient and neutrinos decouple from the cosmic plasma.

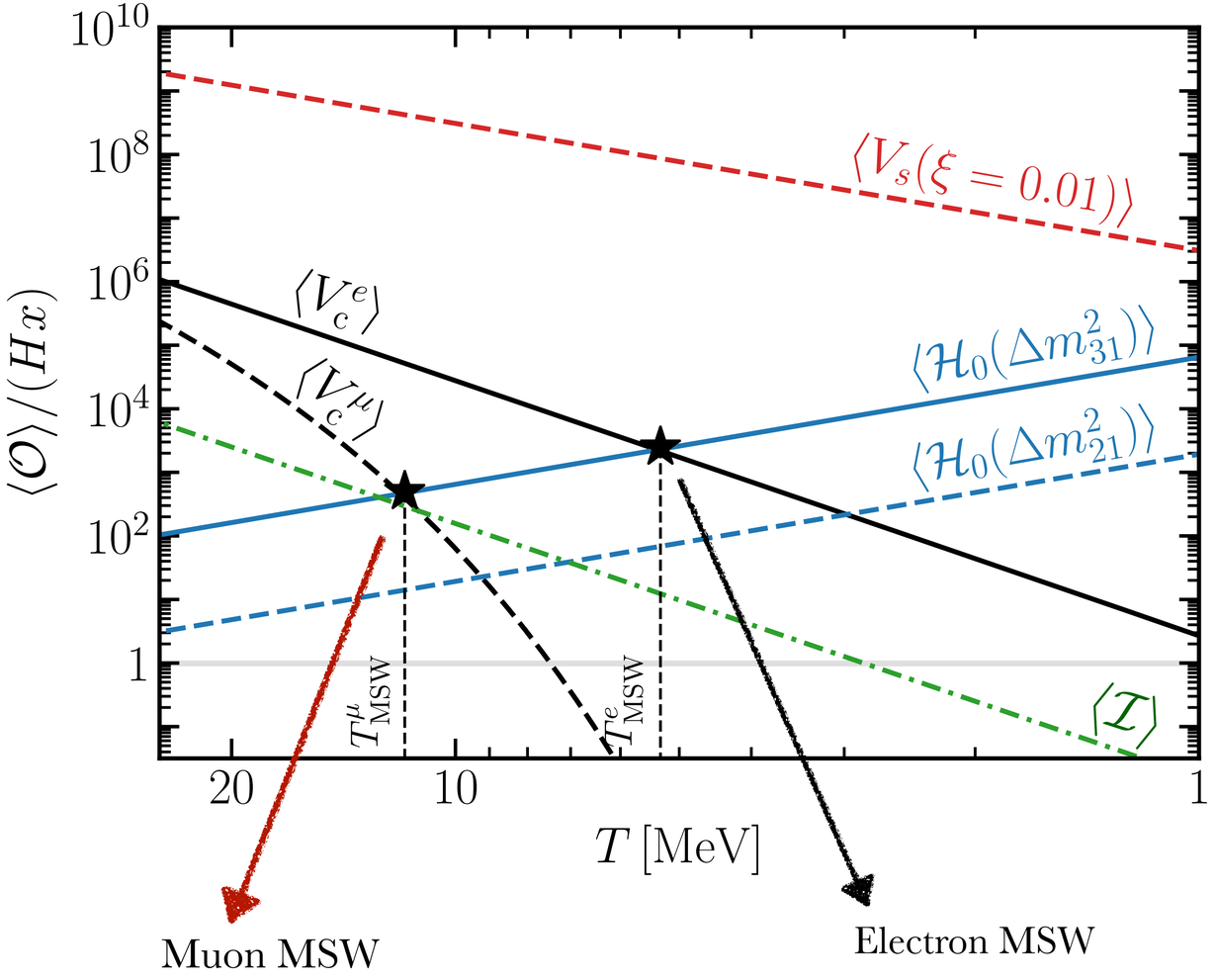

Momentum average

- Therefore, to good accuracy the system can be described with a momentum average ansatz for the density matrices:

$$\rho(t,k) = r(t)\, f_{\rm FD}(y\, T_{\rm cm}/T_\nu, 0)\,, \quad \bar{\rho}(t,k) = \bar{r}(t)\, f_{\rm FD}(y\, T_{\rm cm}/T_\nu, 0)\,,$$

Momentum average

- Therefore, to good accuracy the system can be described with a momentum average ansatz for the density matrices:

$$\rho(t,k) = r(t)\, f_{\rm FD}(y\, T_{\rm cm}/T_\nu, 0)\,, \quad \bar{\rho}(t,k) = \bar{r}(t)\, f_{\rm FD}(y\, T_{\rm cm}/T_\nu, 0)\,,$$

- Then we can integrate in momentum and perform the momentum average: $\langle X \rangle = \dfrac{\int dy y^2 X f_{\rm FD}(y\, T_{\rm cm}/T_\nu, 0)}{\int dy y^2 f_{\rm FD}(y\, T_{\rm cm}/T_\nu, 0)}$

$$\frac{dr}{dt} = -i\left[\langle \mathcal{H}_0 \rangle + \langle V_c \rangle + V_s, r\right] + \langle \mathcal{I} \rangle\,, \qquad \frac{d\bar{r}}{dt} = +i\left[\langle \mathcal{H}_0 \rangle + \langle V_c \rangle - V_s, \bar{r}\right] + \langle \bar{\mathcal{I}} \rangle\,,$$

Momentum average

- Therefore, to good accuracy the system can be described with a momentum average ansatz for the density matrices:

$$\rho(t,k) = r(t)\, f_{\rm FD}(y\, T_{\rm cm}/T_\nu, 0)\,, \quad \bar{\rho}(t,k) = \bar{r}(t)\, f_{\rm FD}(y\, T_{\rm cm}/T_\nu, 0)\,,$$

- Then we can integrate in momentum and perform the momentum average: $\langle X \rangle = \dfrac{\int dy y^2 X f_{\rm FD}(y\, T_{\rm cm}/T_\nu, 0)}{\int dy y^2 f_{\rm FD}(y\, T_{\rm cm}/T_\nu, 0)}$

$$\frac{dr}{dt} = -i\left[\langle \mathcal{H}_0 \rangle + \langle V_c \rangle + V_s, r\right] + \langle \mathcal{I} \rangle\,, \qquad \frac{d\bar{r}}{dt} = +i\left[\langle \mathcal{H}_0 \rangle + \langle V_c \rangle - V_s, \bar{r}\right] + \langle \bar{\mathcal{I}} \rangle\,,$$

- Finally, track the energy transfer between neutrinos and the $e^\pm - \gamma$ plasma via the continuity equation (necessary for a precise computation of $N_{\rm eff}$):

$$\frac{d(\varepsilon_\gamma + \varepsilon_e)}{dt} + 4H\varepsilon_\gamma + 3H(\varepsilon_e + p_e) = -\frac{\delta\varepsilon}{\delta t}\,, \quad \frac{d\varepsilon_\nu}{dt} + 4H\varepsilon_\nu = \frac{\delta\varepsilon}{\delta t}\,,$$

COsmological evolution of lepton FLavour ASYmmetries (COFLASY)

- Code to solve numerically the system of QKEs: https://github.com/mariofnavarro/COFLASY
- Two versions: COFLASY-M (Mathematica) and COFLASY-C (C++)

- Collisions in the momentum average ansatz $\langle \mathcal{I} \rangle$:
  - Analytical form possible in the limit $m_e \to 0$ (COFLASY-M)
  - Numerical integration and interpolation to include m_e effects (COFLASY-C)
  - Alternatively: damping approximation respecting μ-τ $U(2)$, MB statistics…

- Execution times for large initial asymmetries $\xi_\alpha \gtrsim \mathcal{O}(1)$ →
  - COFLASY-C: ~ 30 seconds
  - COFLASY-M: ~ 3 minutes
  - Momentum-dependent code: $\mathcal{O}(10^3)$ slower ~ several hours

[Froustey and Pitrou '21, '24]

Results : Normal Ordering

$$\Delta n_e^{\rm ini} + \Delta n_\mu^{\rm ini} + \Delta n_\tau^{\rm ini} = 0 \qquad \Delta n_\alpha^{\rm ini} = \frac{1}{6}\left(\xi_\alpha^{\rm ini} + \frac{(\xi_\alpha^{\rm ini})^3}{\pi^2}\right)$$

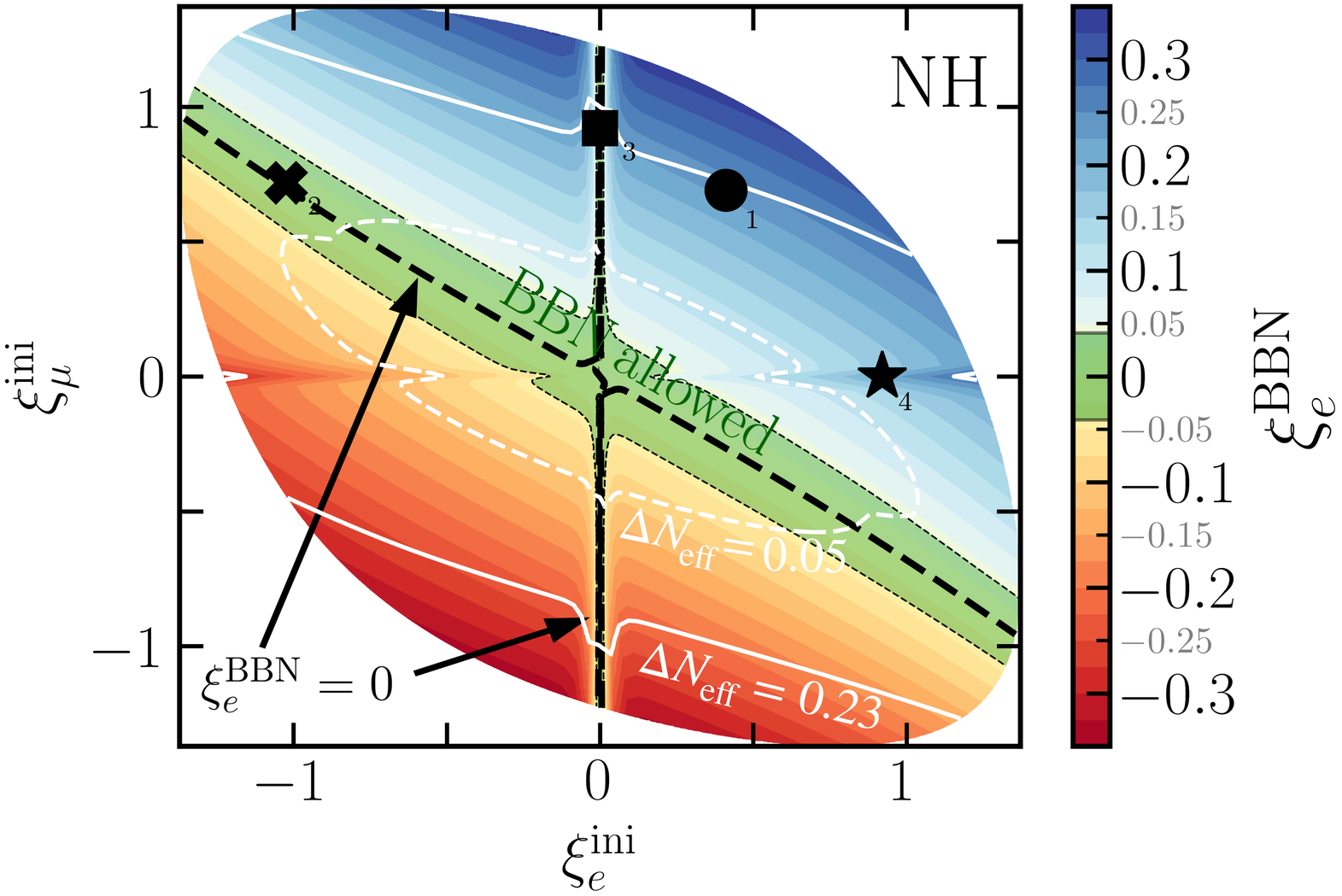

Results : Normal Ordering

$$\Delta n_e^{\rm ini} + \Delta n_\mu^{\rm ini} + \Delta n_\tau^{\rm ini} = 0 \qquad \Delta n_\alpha^{\rm ini} = \frac{1}{6}\left(\xi_\alpha^{\rm ini} + \frac{(\xi_\alpha^{\rm ini})^3}{\pi^2}\right)$$

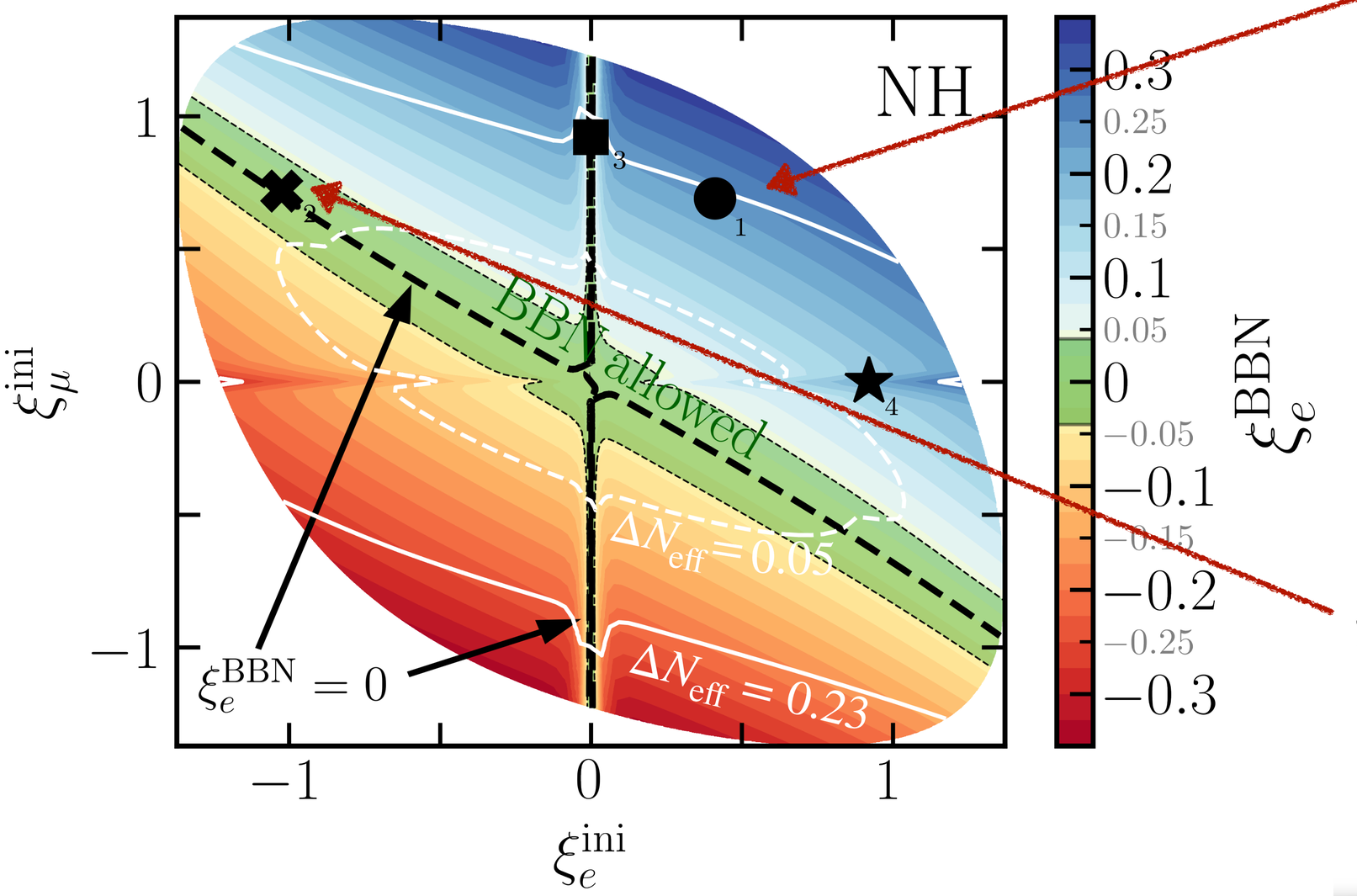

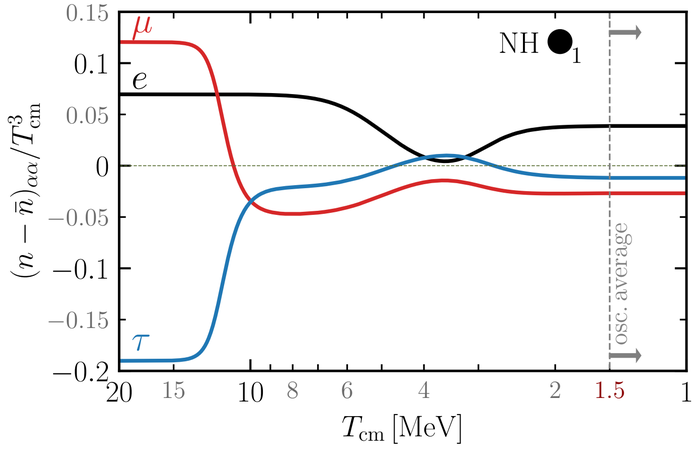

Smooth (adiabatic) behaviour leads to flavour equilibration for:

$$\xi_e^{\rm ini} \approx -\frac{2}{3}\xi_\mu^{\rm ini}\,, \quad \xi_\tau^{\rm ini} \approx -\frac{1}{3}\xi_\mu^{\rm ini}\,,$$

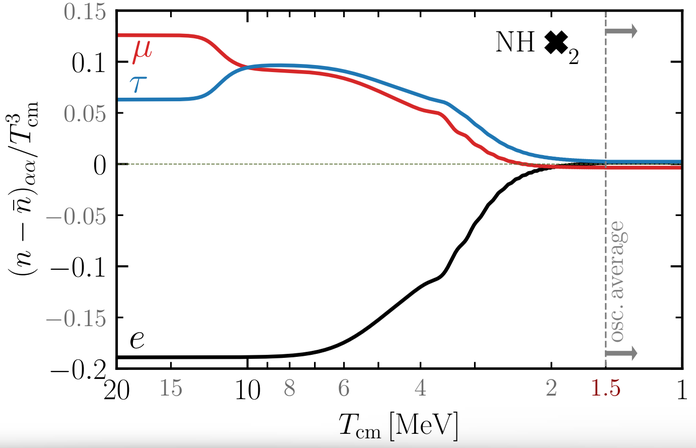

Results : Normal Ordering

$$\Delta n_e^{\rm ini} + \Delta n_\mu^{\rm ini} + \Delta n_\tau^{\rm ini} = 0 \qquad \Delta n_\alpha^{\rm ini} = \frac{1}{6}\left(\xi_\alpha^{\rm ini} + \frac{(\xi_\alpha^{\rm ini})^3}{\pi^2}\right)$$

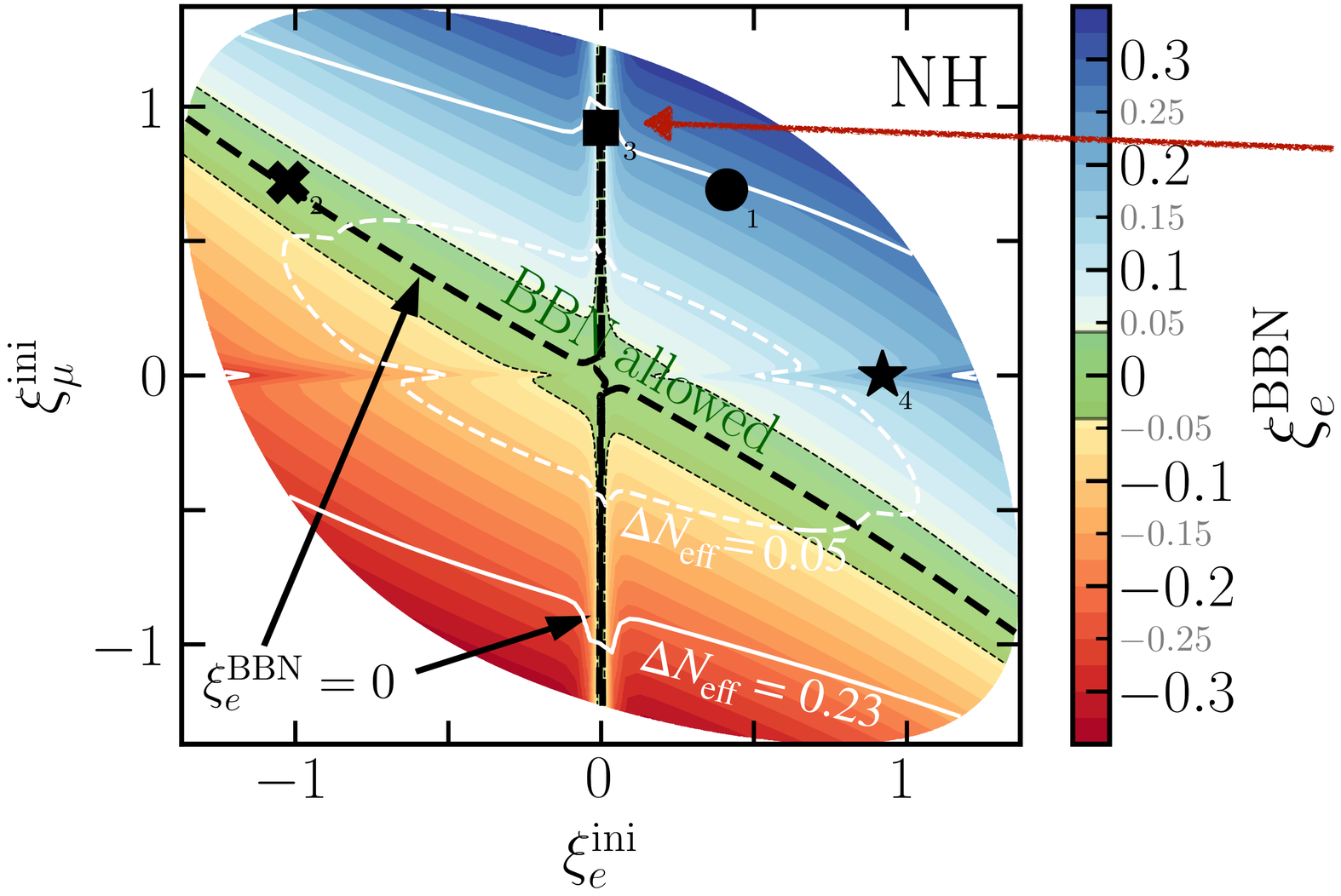

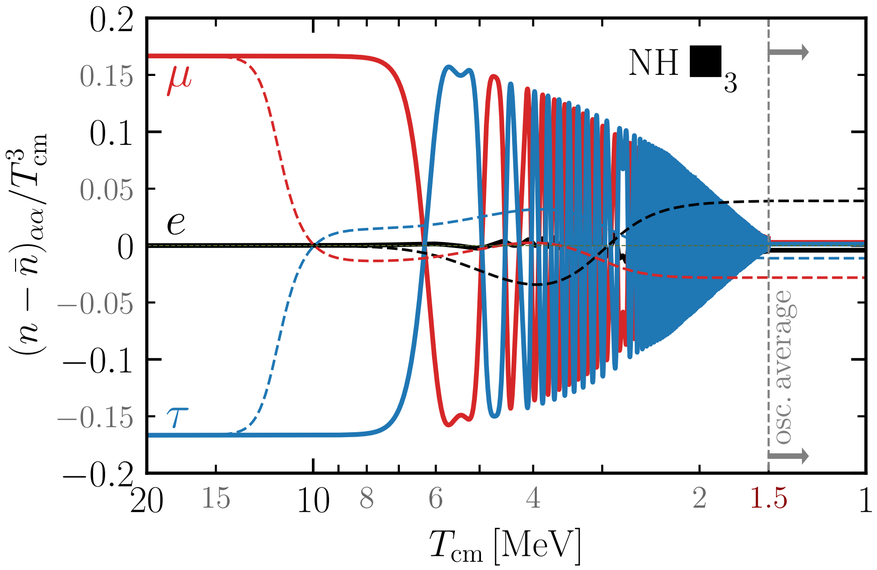

Non-adiabatic muon MSW leads to flavour equilibration:

$$\xi_e^{\rm ini} \simeq 0\,, \quad \xi_\mu^{\rm ini} \simeq -\xi_\tau^{\rm ini}$$

Results : Normal Ordering

$$\Delta n_e^{\rm ini} + \Delta n_\mu^{\rm ini} + \Delta n_\tau^{\rm ini} = 0 \qquad \Delta n_\alpha^{\rm ini} = \frac{1}{6}\left(\xi_\alpha^{\rm ini} + \frac{(\xi_\alpha^{\rm ini})^3}{\pi^2}\right)$$

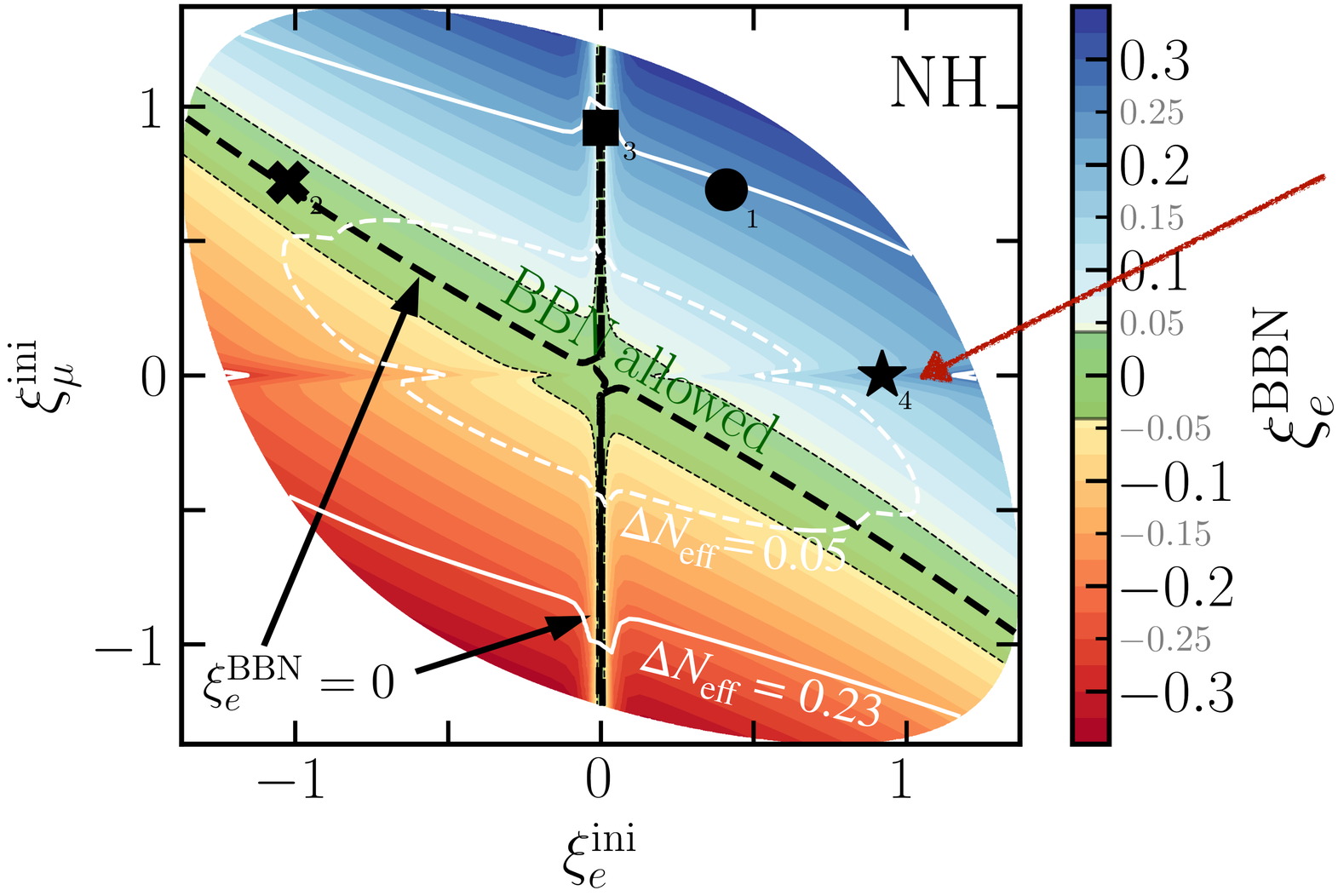

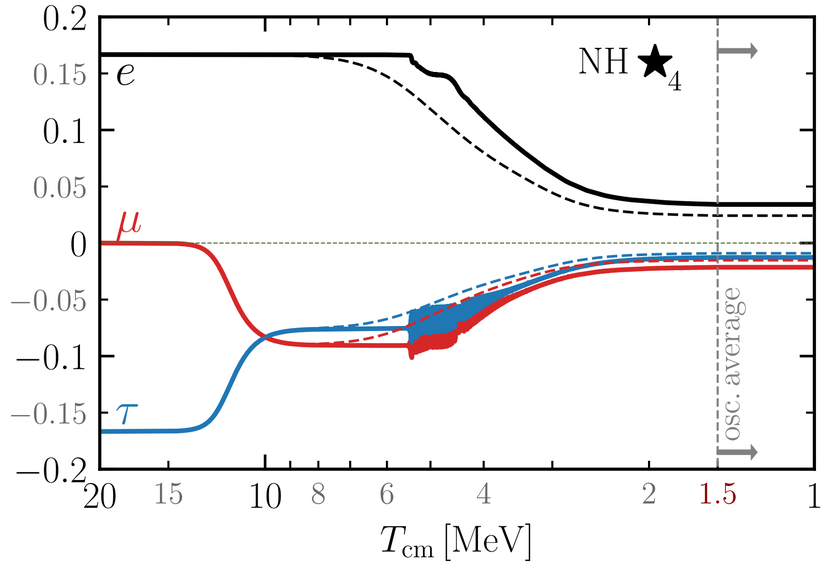

Non-adiabatic electron MSW leads to less washout:

$$\xi_e^{\rm ini} \simeq -\xi_\tau^{\rm ini}\,, \quad \xi_\mu^{\rm ini} \simeq 0$$

- $\Delta N_{\rm eff}$ not competitive (yet)

Results: Inverted Ordering

$$\Delta n_e^{\rm ini} + \Delta n_\mu^{\rm ini} + \Delta n_\tau^{\rm ini} = 0 \qquad \Delta n_\alpha^{\rm ini} = \frac{1}{6}\left(\xi_\alpha^{\rm ini} + \frac{(\xi_\alpha^{\rm ini})^3}{\pi^2}\right)$$

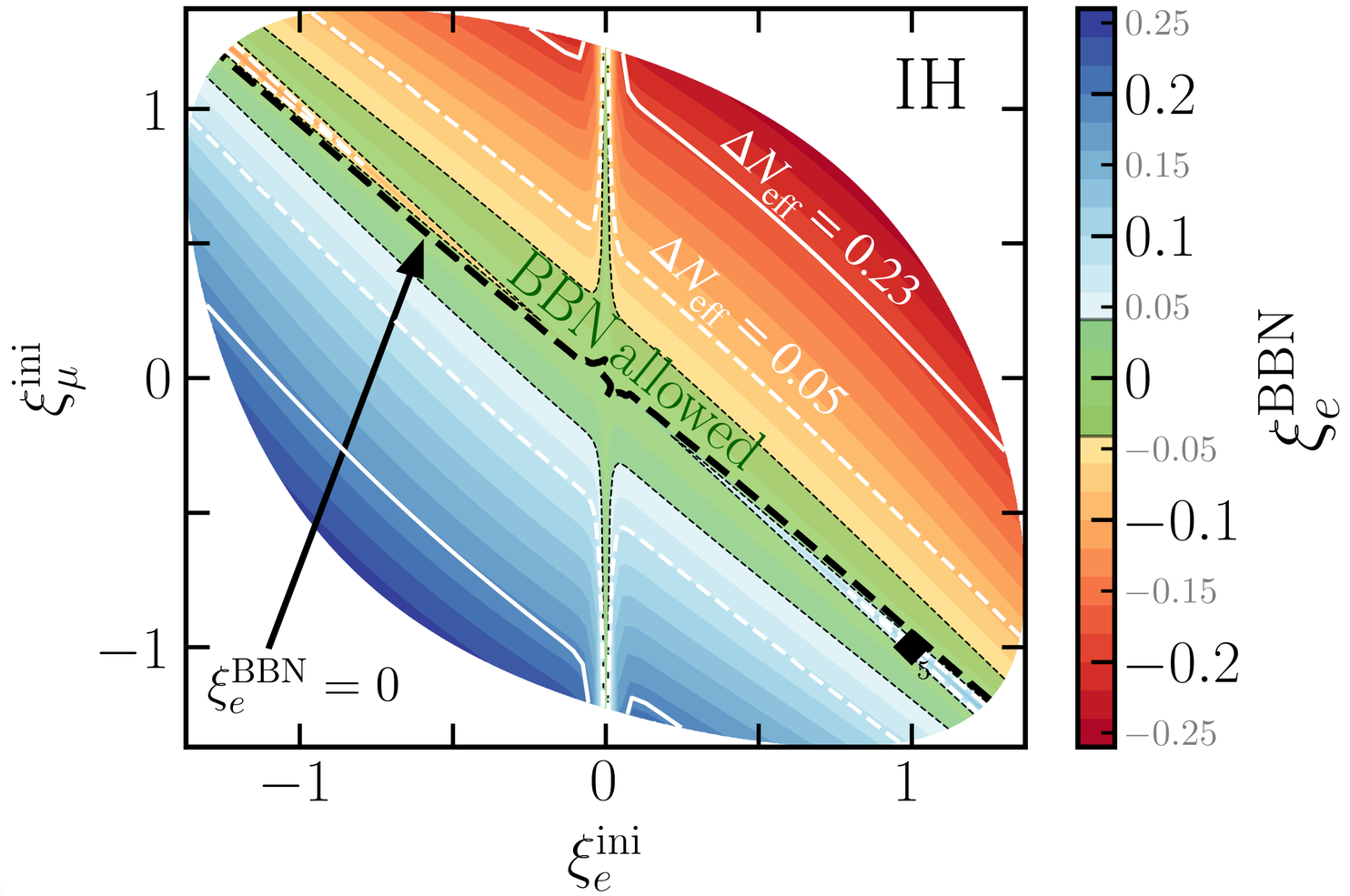

Results: Inverted Ordering

$$\Delta n_e^{\rm ini} + \Delta n_\mu^{\rm ini} + \Delta n_\tau^{\rm ini} = 0 \qquad \Delta n_\alpha^{\rm ini} = \frac{1}{6}\left(\xi_\alpha^{\rm ini} + \frac{(\xi_\alpha^{\rm ini})^3}{\pi^2}\right)$$

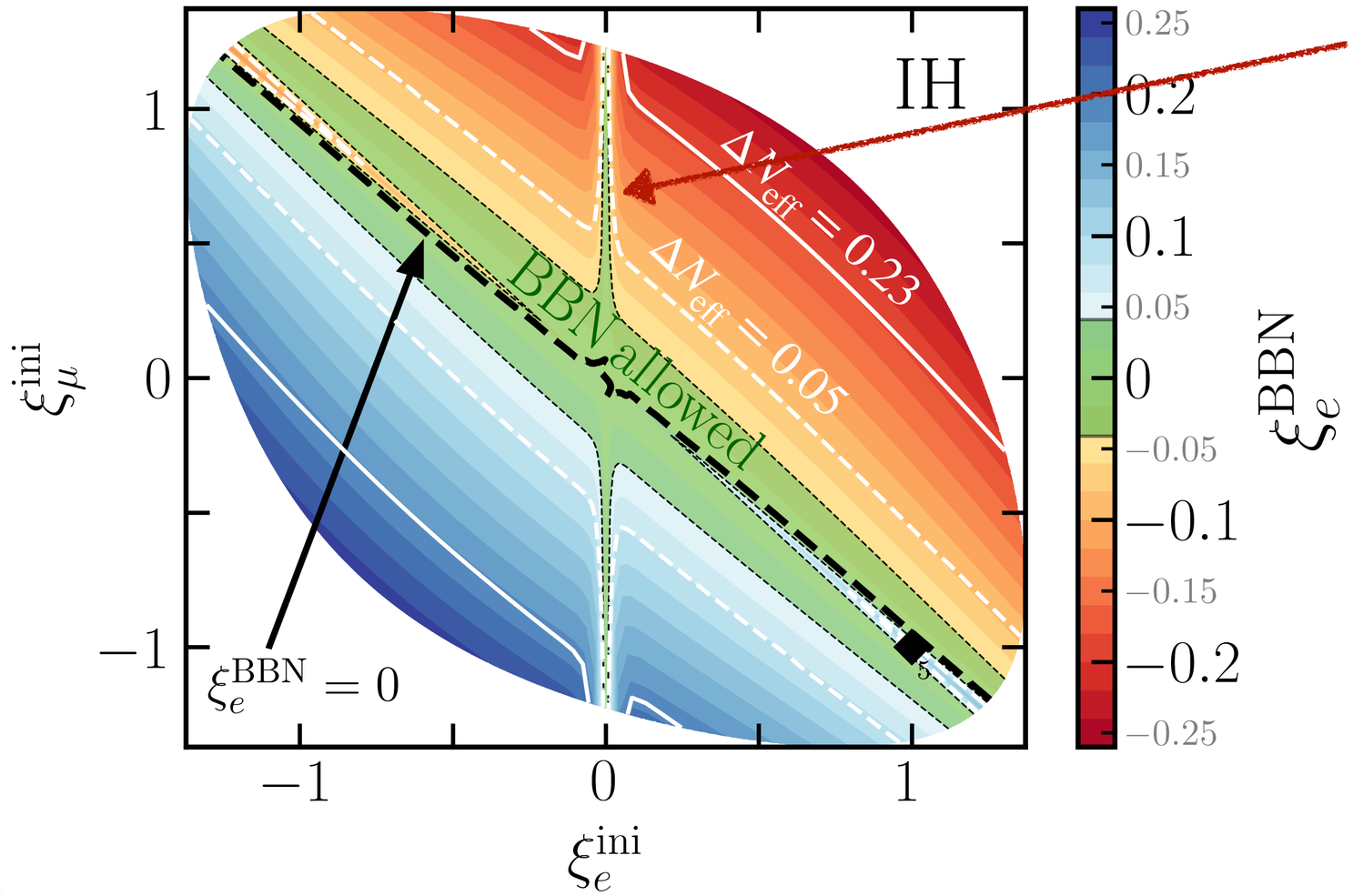

- Non-adiabatic muon MSW as in NH:

$$\xi_e^{\rm ini} \simeq 0\,, \quad \xi_\mu^{\rm ini} \simeq -\xi_\tau^{\rm ini}$$

Results: Inverted Ordering

$$\Delta n_e^{\rm ini} + \Delta n_\mu^{\rm ini} + \Delta n_\tau^{\rm ini} = 0 \qquad \Delta n_\alpha^{\rm ini} = \frac{1}{6}\left(\xi_\alpha^{\rm ini} + \frac{(\xi_\alpha^{\rm ini})^3}{\pi^2}\right)$$

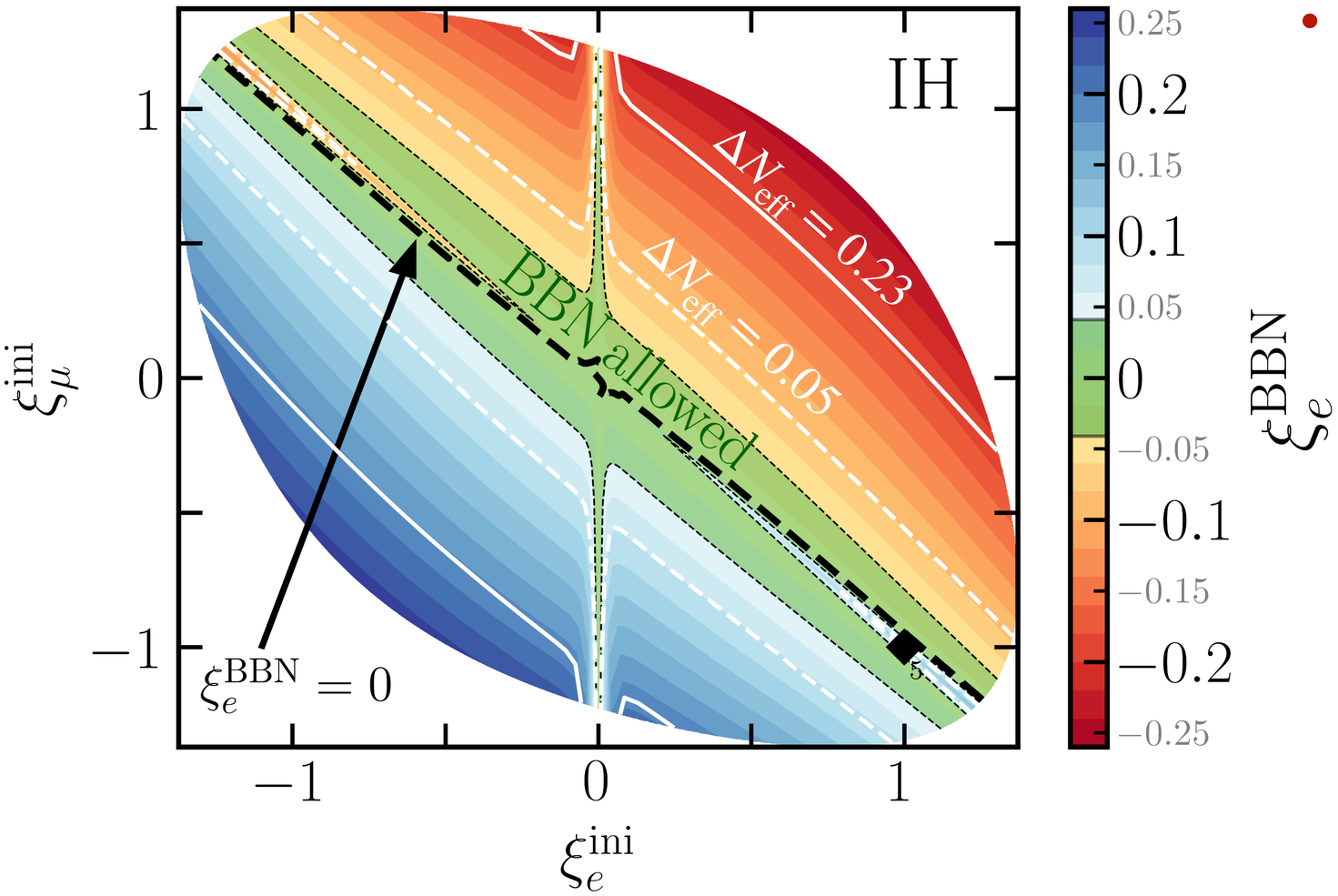

- Adiabatic flavour equilibration generally more efficient than in NH.
- $\Delta N_{\rm eff}$ aligns with BBN band because flavour equilibration is more efficient.

Results: Inverted Ordering

$$\Delta n_e^{\rm ini} + \Delta n_\mu^{\rm ini} + \Delta n_\tau^{\rm ini} = 0 \qquad \Delta n_\alpha^{\rm ini} = \frac{1}{6}\left(\xi_\alpha^{\rm ini} + \frac{(\xi_\alpha^{\rm ini})^3}{\pi^2}\right)$$

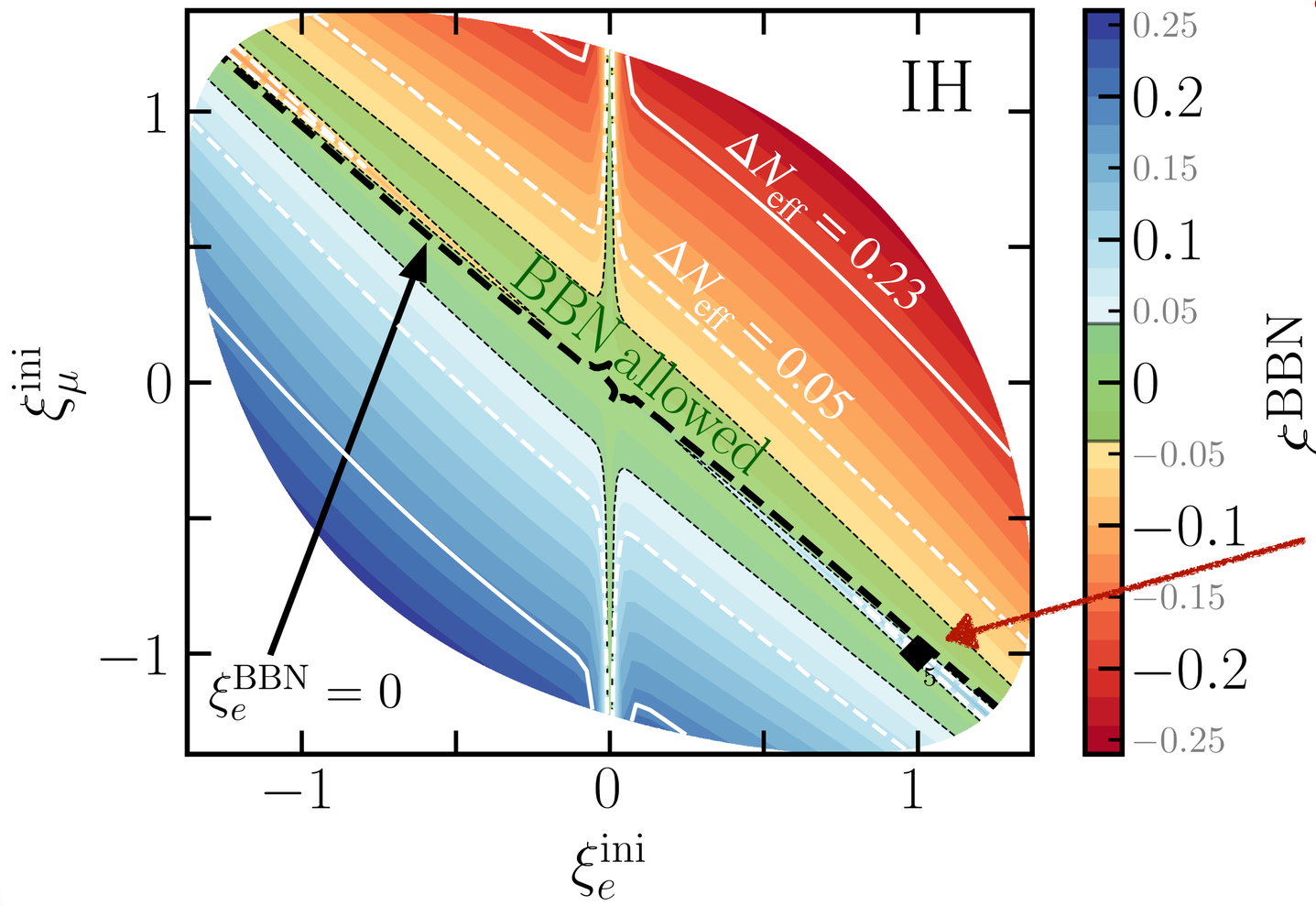

- Adiabatic flavour equilibration generally more efficient than in NH.
- But maximal adiabatic washout close to non-adiabatic *e*-MSW (now in $\xi_\tau = 0$ direction)

$$\xi_e^{\rm ini} \simeq -\xi_\mu^{\rm ini}\,, \quad \xi_\tau^{\rm ini} \simeq 0$$

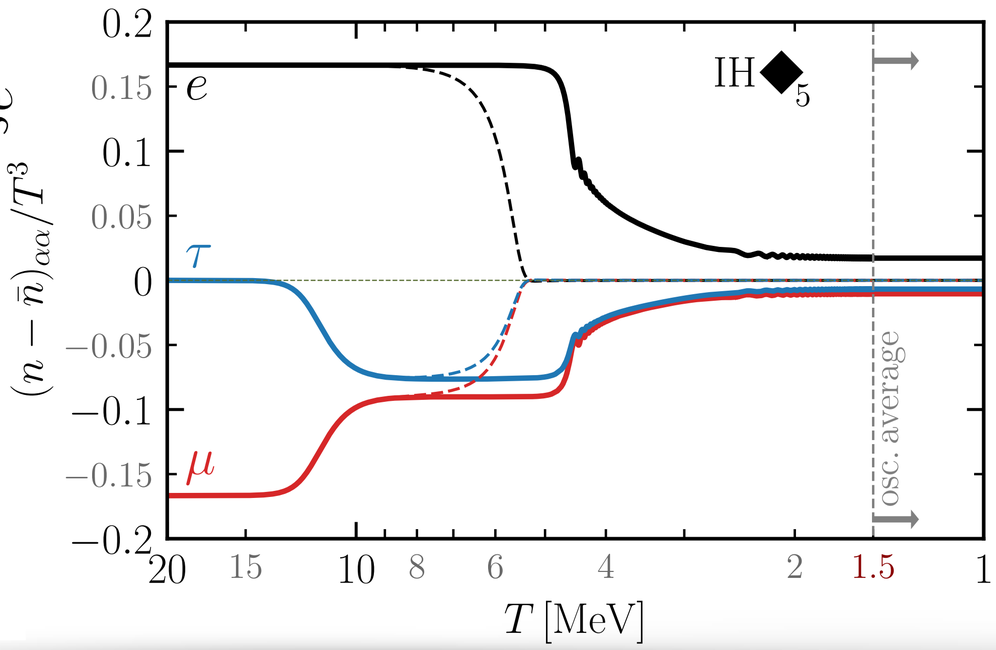

Early Universe implications

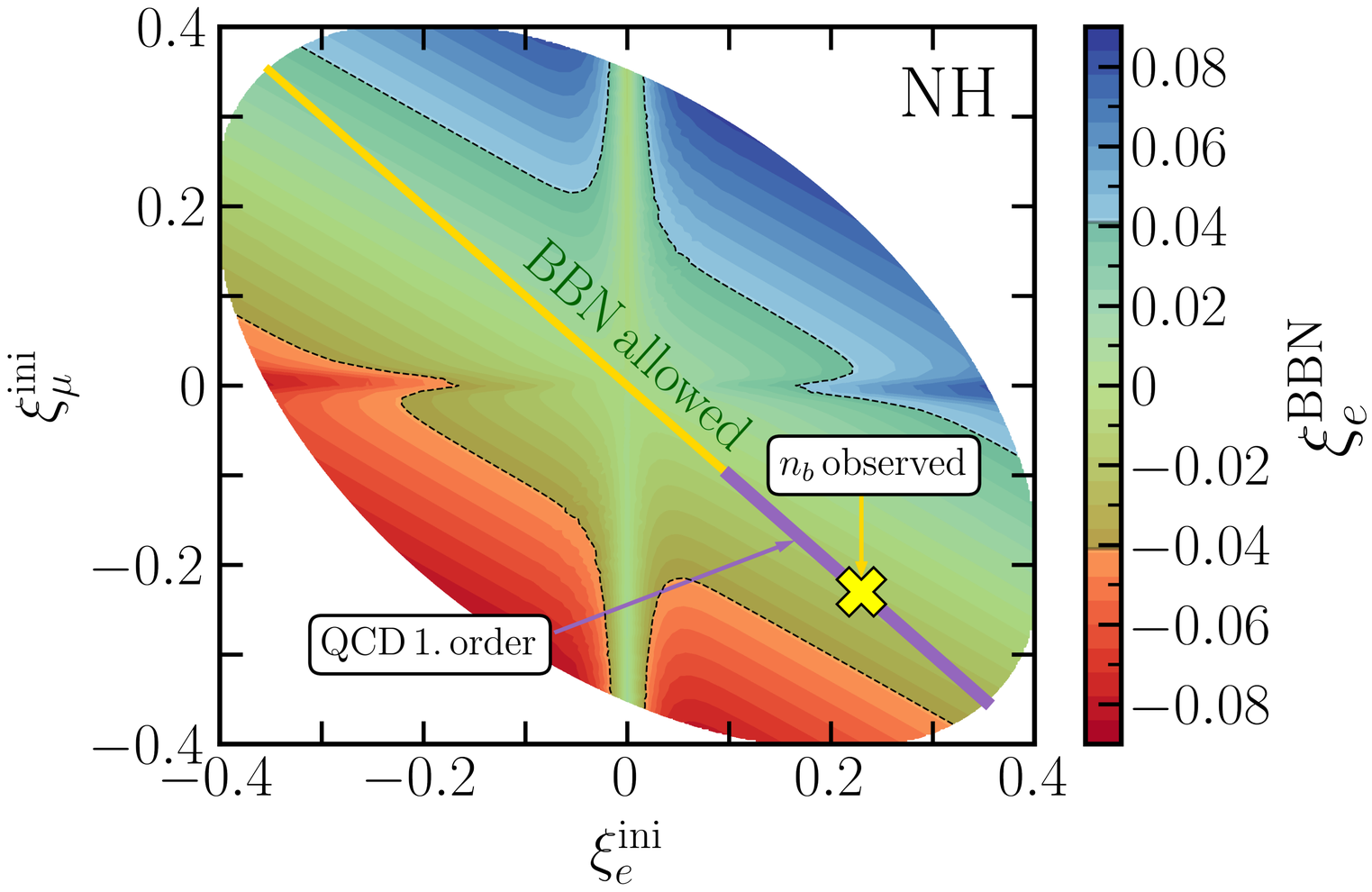

1st order QCD phase transition

$$\xi_e^{\rm ini} = -\xi_\mu^{\rm ini} \gtrsim 0.1\,, \quad \xi_\tau \approx 0$$

[Gao and Oldengott, '21]

Leptoflavourgenesis

$$\xi_e^{\rm ini} = -\xi_\mu^{\rm ini} \approx 0.23\,, \quad \xi_\tau \approx 0$$

[Mukaida, Schmitz, Yamada, '21]

Our results NH (adiabatic)

$$\xi_e^{\rm ini} = -\xi_\mu^{\rm ini} \lesssim 0.5$$

Early Universe implications

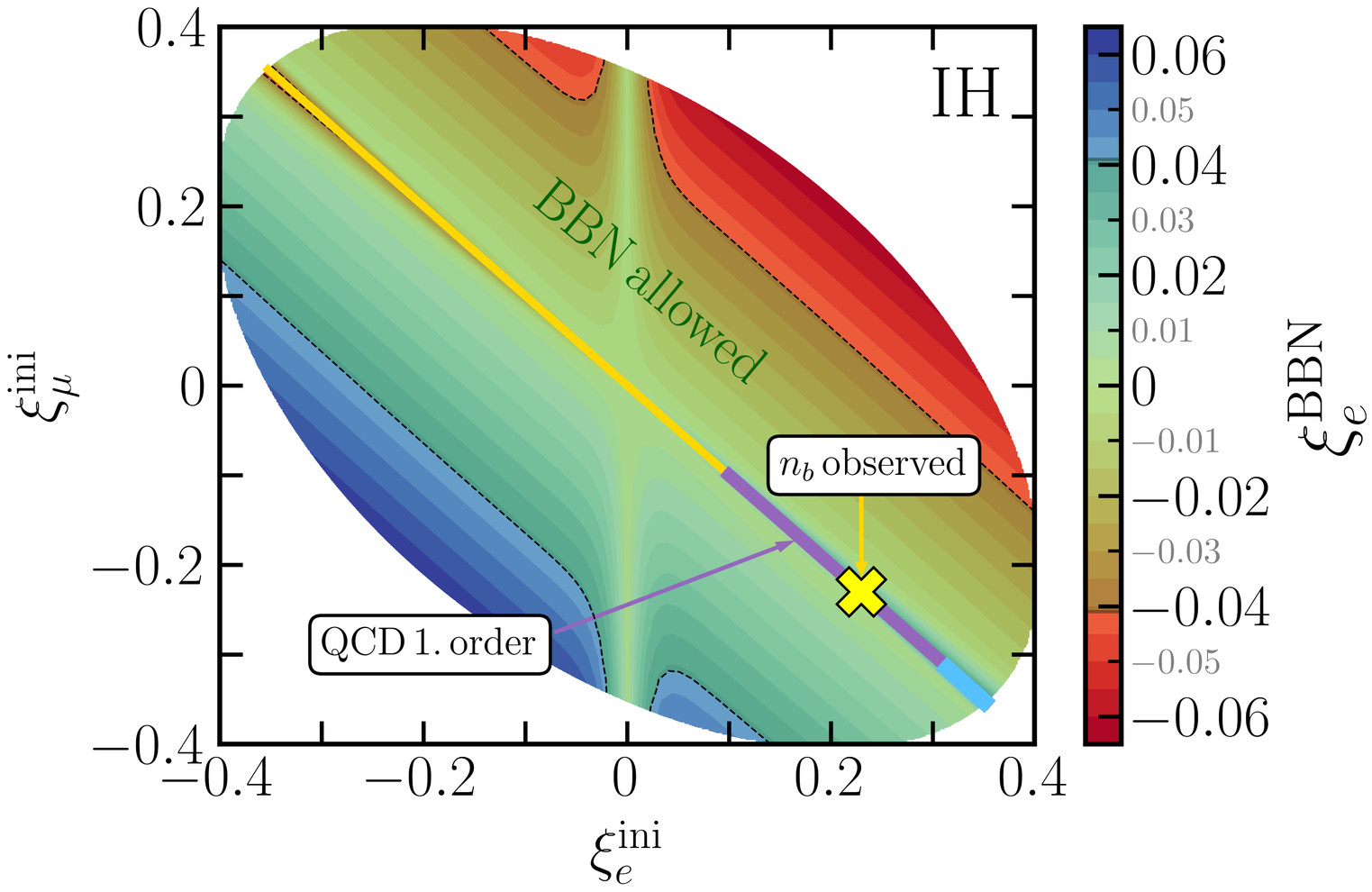

1st order QCD phase transition

$$\xi_e^{\rm ini} = -\xi_\mu^{\rm ini} \gtrsim 0.1\,, \quad \xi_\tau \approx 0$$

[Gao and Oldengott, '21]

Leptoflavourgenesis

$$\xi_e^{\rm ini} = -\xi_\mu^{\rm ini} \approx 0.23\,, \quad \xi_\tau \approx 0$$

[Mukaida, Schmitz, Yamada, '21]

Our results IH (non-adiabatic *e*-MSW)

$$\xi_e^{\rm ini} = -\xi_\mu^{\rm ini} \lesssim 0.3$$

Global analysis: total lepton number

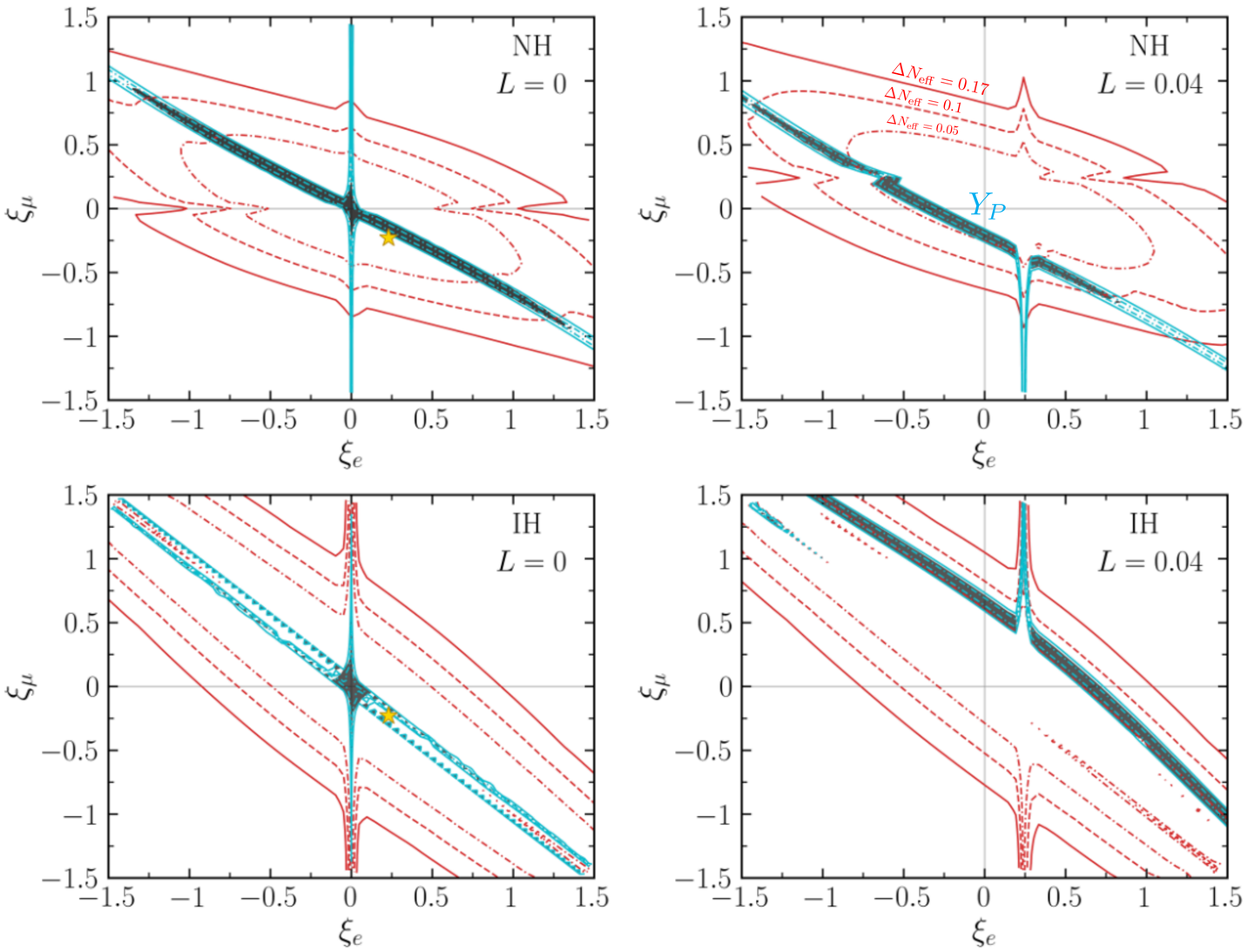

current 95% CL

$$-0.10(0.08) \leq L \leq 0.10(0.08)$$

future (Simon's observatory)

$$-0.06(0.05) \leq L \leq 0.07(0.06)$$

NH(IH)

Take home messages

- Lepton flavour asymmetries are well motivated from early Universe scenarios

- We present a fast and reliable formalism to evolve lepton flavour asymmetries from the onset of neutrino oscillations to BBN times:

$$(\xi_e, \xi_\mu, \xi_\tau) \rightarrow \texttt{COFLASY} \rightarrow (\xi_e^{\rm BBN}, \Delta N_{\rm eff}, Y_p)$$

- COFLASY-M (Mathematica)
- COFLASY-C (C++)

1. For $L \approx 0$, we uncover that only specific flavour directions are compatible with data
2. Leptoflavourgenesis and QCD 1st order transition are allowed but close to current bounds
3. We present a global bound on total lepton number in the Universe from BBN and CMB

$$-0.10(0.08) \leq L \leq 0.10(0.08) \qquad \text{NH(IH)}$$

Global analysis: total lepton number

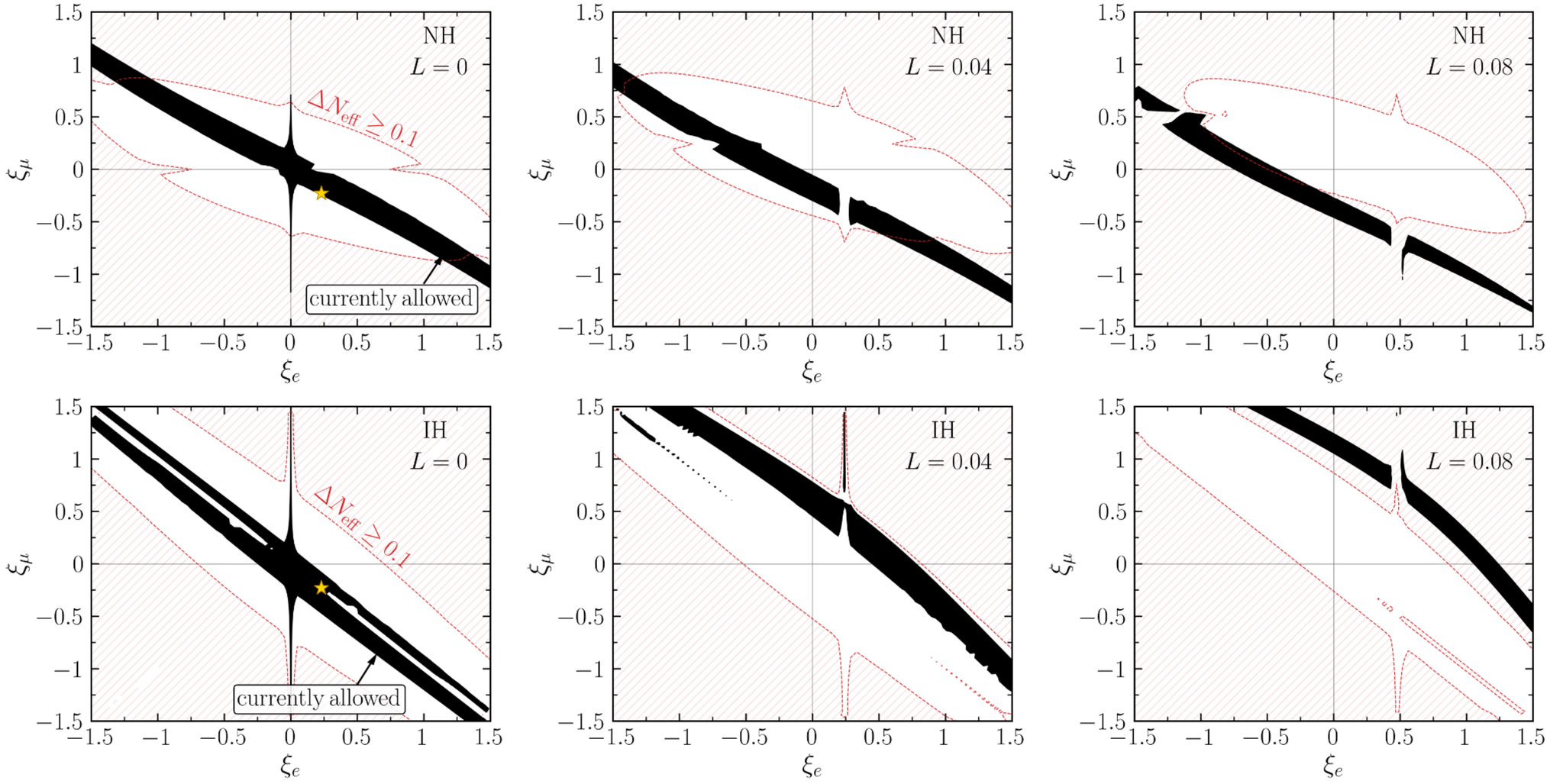

future (mostly Simon's observatory)

$$-0.12\,(0.10) \leq L \leq 0.13\,(0.12) \quad \longrightarrow \quad -0.06(0.05) \leq L \leq 0.07(0.06) \quad \text{NH(IH)}$$

Backup: IH washout and $L \neq 0$

Decompose the initial asymmetry schematically as

$$\vec{\xi}_{\rm ini} = \vec{\xi}_{\rm trace} + \vec{\xi}_{\rm comp},$$

Backup: Comparison with momentum-dependent

- Dataset of about 2300 points computed with full momentum-dependent code by Froustey and Pitrou [2405.06509]:

$$\delta n_\alpha \equiv \max\left[\left|\frac{(n-\bar{n})^{\text{this work}}_{\alpha\alpha}}{(n-\bar{n})^{\text{Froustey+}}_{\alpha\alpha}}\right|, \left|\frac{(n-\bar{n})^{\text{Froustey+}}_{\alpha\alpha}}{(n-\bar{n})^{\text{this work}}_{\alpha\alpha}}\right|\right] - 1\Bigg|_{\text{BBN}},$$

- 85% of points → $\delta n_\alpha \leq 1$ out of this 47%(11%) → $\delta n_\alpha \leq 0.1(0.01)$

- From the remaining 15% which show poor agreement, 83% are excluded

- Focusing on the points allowed (at 95% CL), we find that the deviation from the momentum-dependent code is well modeled by a Gaussian distribution with zero mean and a standard deviation of 0.016:

$$\xi_e^{\text{BBN}} = 0.001 \pm 0.013\ (\text{exp}) \pm 0.016\ (\text{th}) \quad (@\,1\sigma)\,,$$

Backup: $\xi_e^{\rm BBN}$ explain

- Electron neutrino chemical potential connected numerically to helium and deuterium abundances, see e.g. Pitrou *et al* [1801.08023], Froustey and Pitrou [2405.06509]:

The net effect on helium-4 and deuterium abundances coming from an electron (anti)neutrino chemical potential during BBN was estimated numerically in [27]:

$$\frac{Y_{\rm p}}{Y_{\rm p}|_{\xi_e=0}} \simeq e^{-0.96\xi_e^{\rm BBN}} \,, \quad \frac{\rm D/H}{\rm D/H|_{\xi_e=0}} \simeq e^{-0.53\xi_e^{\rm BBN}} \,. \quad (16)$$

$$\begin{aligned} \xi_e^{\rm BBN} \sim \left[\frac{6(n_e-\bar{n}_e)}{T_\gamma^3}\right]_{\rm FO} &= \left[\frac{6(n_e-\bar{n}_e)}{z^3 T_{\rm cm}^3}\right]_{\rm FO} \\ &= 6\left[\frac{\eta_e}{z^3}\right]_{\rm FO} \\ &= 6\left[\frac{\eta_e}{z^3}\right]_{\rm final} \times \left(\frac{z_{\rm final}}{z_{\rm FO}}\right)^3 \,, \end{aligned} \quad (17)$$

Backup: Comparison with momentum-dependent

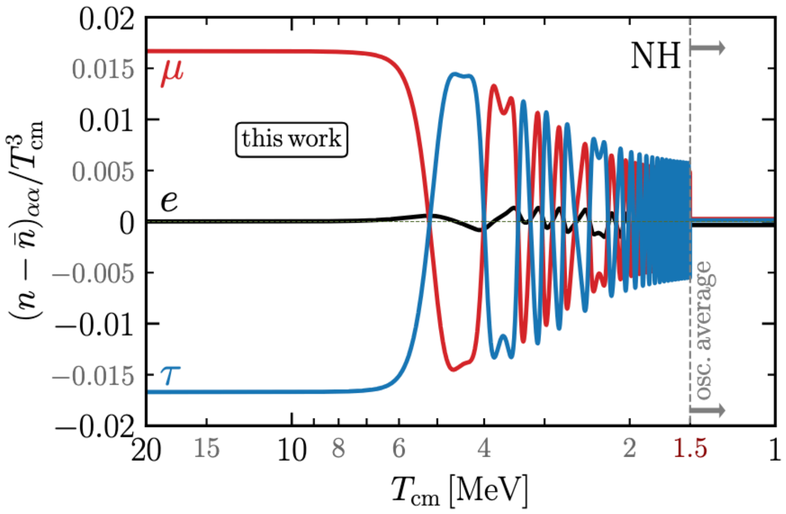

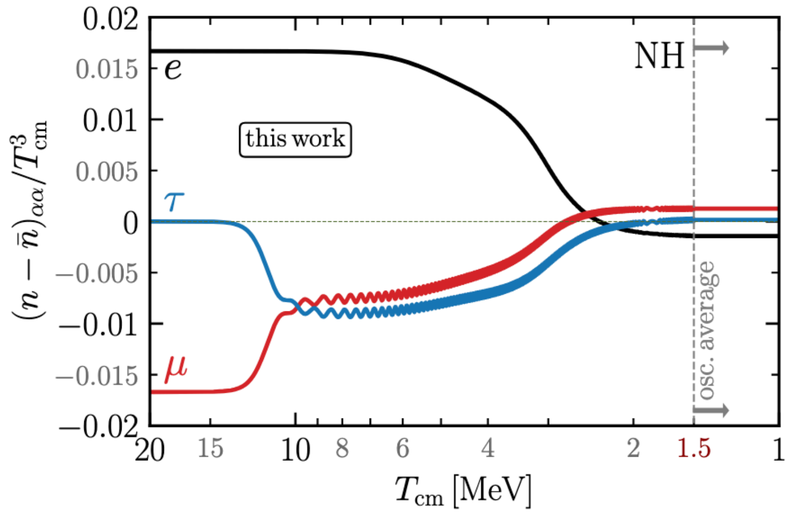

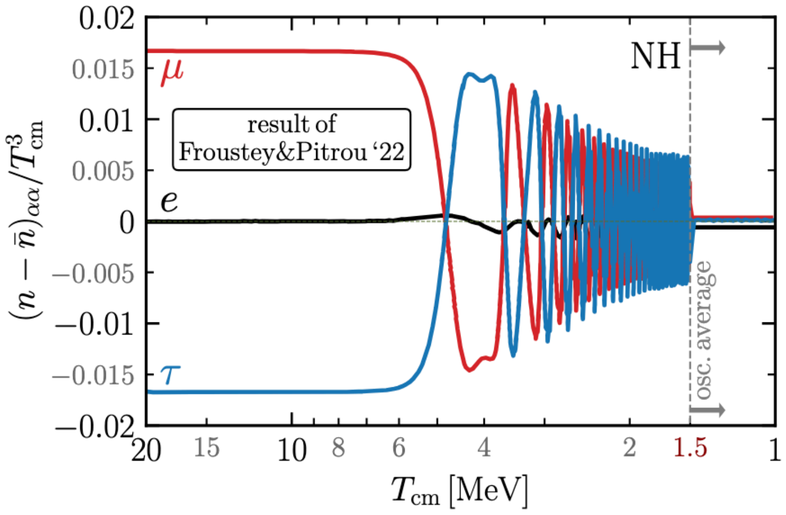

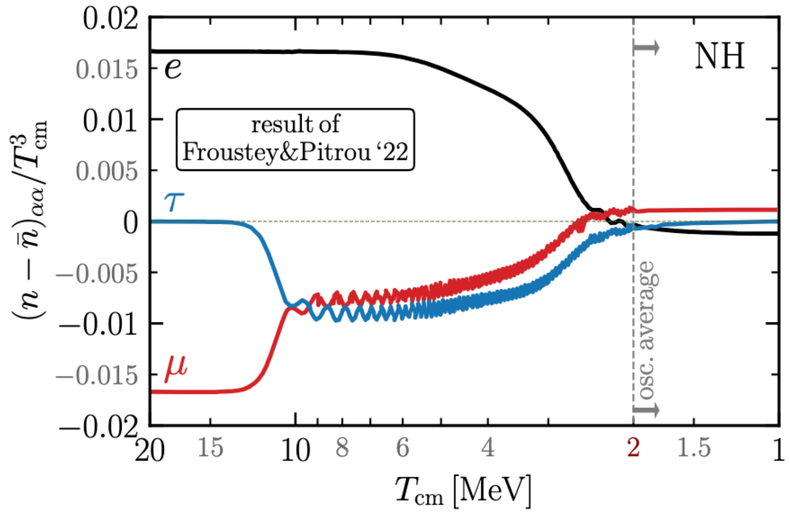

Backup: Comparison with momentum-dependent

- Dataset of about 2300 points computed with full momentum-dependent code by Froustey and Pitrou [2405.06509]:

$$\delta N_{\rm eff} \equiv \max\left[\left|\frac{\Delta N_{\rm eff}^{\text{this work}}}{\Delta N_{\rm eff}^{\text{Froustey+}}}\right|, \left|\frac{\Delta N_{\rm eff}^{\text{Froustey+}}}{\Delta N_{\rm eff}^{\text{this work}}}\right|\right] - 1 \Bigg|_{T_{\rm cm}=0.006\,\text{MeV}},$$

- 99% of points → $\delta N_{\rm eff} \leq 1$ out of this 60% (1%) → $\delta N_{\rm eff} \leq 0.1(0.01)$

- We conclude that in this case the theoretical uncertainty is subdominant compared to current experimental uncertainty.

Backup: BBN

$$T_{\nu_e}/T_\gamma = \left(\frac{\frac{\rho_{\nu_e}+\rho_{\bar{\nu}_e}}{T_{\rm cm}^4}}{2\frac{7}{8}\frac{\pi^2}{30}} \right)^{1/4} \frac{1}{z_\gamma}\,, \tag{2.21a}$$

$$\xi_e = 6 \times \frac{n_{\nu_e} - n_{\bar{\nu}_e}}{T_{\rm cm}^3} \times \left(\frac{\frac{\rho_{\nu_e}+\rho_{\bar{\nu}_e}}{T_{\rm cm}^4}}{2\frac{7}{8}\frac{\pi^2}{30}} \right)^{-3/4}\,, \tag{2.21b}$$

where $(\rho_{\nu_e}+\rho_{\bar{\nu}_e})/T_{\rm cm}^4$, $(n_{\nu_e}-n_{\bar{\nu}_e})/T_{\rm cm}^3$ and z_γ are direct outputs of our solver of the QKEs. We explicitly

$$\frac{Y_{\rm P}}{Y_{\rm P}^{\rm Ref}} = \left[\frac{\Omega_b h^2}{\Omega_b h^2|^{\rm Ref}}\right]^{0.039} \exp\Big\{ -0.961\,\xi_e - 0.185\,\xi_e^2 + 0.001\,\xi_e^3 + 0.053\,\Delta N_{\rm eff} - 0.682\,\delta_T + 0.72\,\delta_T^2 + 0.011\,\xi_e \Delta N_{\rm eff} - 3.5\,\xi_e\delta_T - 0.9\,\xi_e^2\delta_T + 2.2\,\xi_e\delta_T^2 + 0.016\,\Delta N_{\rm eff}\delta_T \Big\}\,, \tag{2.22a}$$

$$\frac{{\rm D/H}|_{\rm P}}{{\rm D/H}|_{\rm P}^{\rm Ref}} = \left[\frac{\Omega_b h^2}{\Omega_b h^2|^{\rm Ref}}\right]^{-1.64} \exp\Big\{ -0.528\,\xi_e + 0.22\,\xi_e^2 - 0.052\,\xi_e^3 + 0.133\,\Delta N_{\rm eff} - 0.378\,\delta_T + 0.562\,\delta_T^2 - 0.026\,\xi_e \Delta N_{\rm eff} - 1.5\,\xi_e\delta_T - 0.0096\,\Delta N_{\rm eff}\delta_T \Big\}\,. \tag{2.22b}$$

Synchronous oscillations

- Easier to understand synchronous oscillations by using the vector representation of hermitian 3×3 matrices.
- Expanding in the basis of $SU(3)$ Gell-Mann matrices:

$$\rho_0 = \mathrm{Tr}(\rho) \qquad \vec{\lambda} = \lambda_i$$

$$\rho = \frac{1}{3}\rho_0 \mathbb{I} + \frac{1}{2}\vec{\rho}\cdot\vec{\lambda} \qquad \vec{\rho} = \mathrm{Tr}(\rho\lambda_i) \qquad i = 1, ..., 8$$

- Similar for all contributions to the QKEs: $\mathcal{H}_0 \to \vec{\mathcal{H}}_0\,, \qquad V_c \to \vec{V}_c$

Synchronous oscillations

- Easier to understand synchronous oscillations by using the vector representation of hermitian 3×3 matrices.
- Expanding in the basis of $SU(3)$ Gell-Mann matrices:

$$\rho_0 = \mathrm{Tr}(\rho) \qquad \vec{\lambda} = \lambda_i$$

$$\rho = \frac{1}{3}\rho_0 \mathbb{I} + \frac{1}{2}\vec{\rho}\cdot\vec{\lambda} \qquad \vec{\rho} = \mathrm{Tr}(\rho\lambda_i) \qquad i = 1, ..., 8$$

- Similar for all contributions to the QKEs: $\mathcal{H}_0 \to \vec{\mathcal{H}}_0\,, \qquad V_c \to \vec{V}_c$

[Pastor, Raffelt, Semikoz '01, Froustey and Pitrou '21 ...]

- The evolution of all momentum modes is locked on the evolution of the asymmetry vector, which precesses around $\vec{\mathcal{H}}_0(y_{\rm eff}) + \vec{V}_c(y_{\rm eff})$ with effective momentum $y_{\rm eff} \approx \pi$:

$$\vec{\mathcal{A}} = \int \frac{d^3k'}{(2\pi)^3}(\vec{\rho} - \bar{\vec{\rho}})$$

$$\boxed{\frac{d\vec{\mathcal{A}}}{dt} = \mathcal{F} y_{\rm eff}\left[\vec{\mathcal{H}}_0(y_{\rm eff}) + \vec{V}_c(y_{\rm eff})\right] \times \vec{\mathcal{A}}} \qquad y = \frac{k}{T}$$

Synchronous oscillations

$$\xi_\mu^{\rm ini} = 0.1\,, \quad \xi_e^{\rm ini} = \xi_\tau^{\rm ini} = 0$$

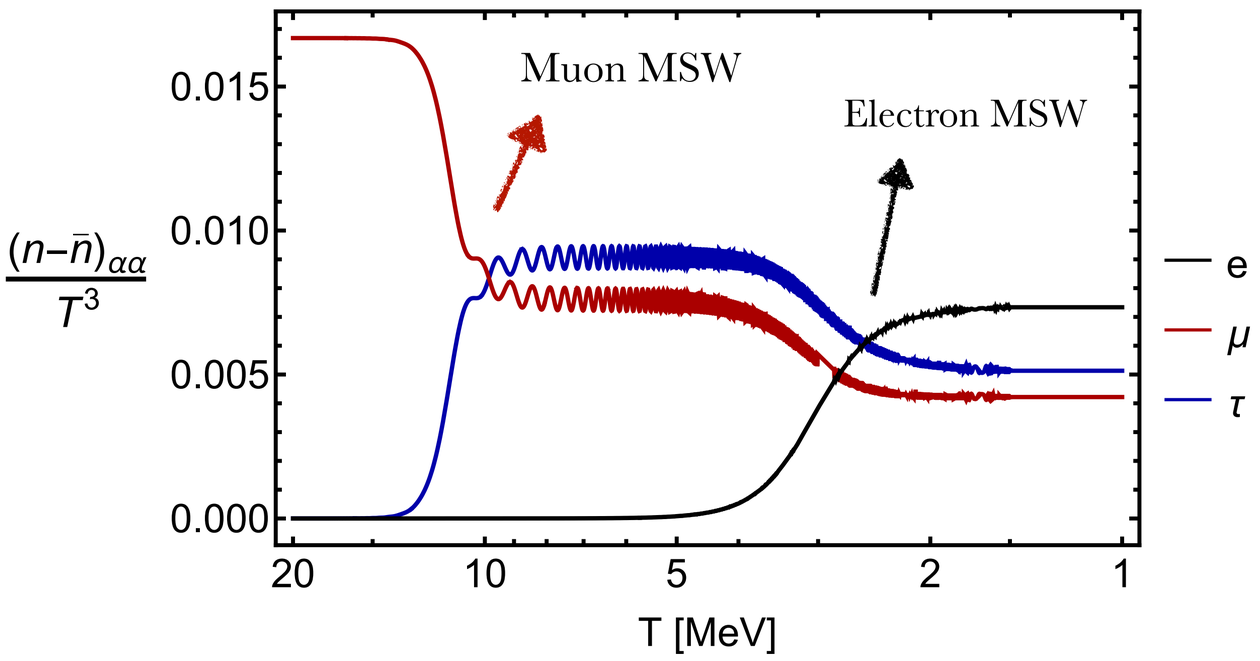

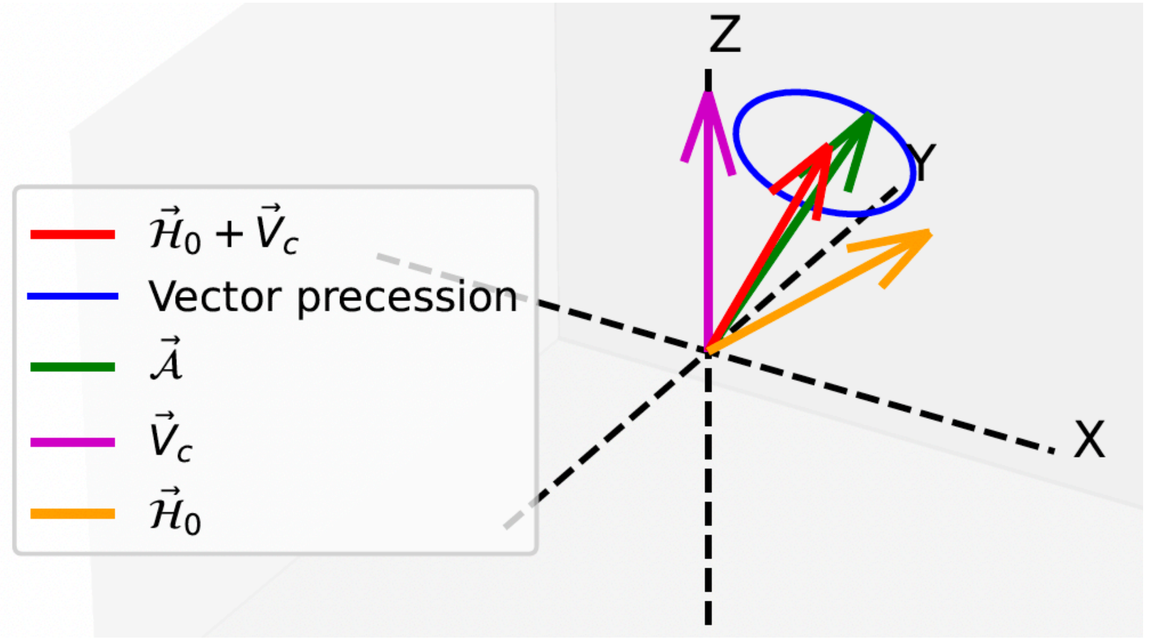

[Pastor, Raffelt, Semikoz '01, Froustey and Pitrou '21 …]

$$\vec{\mathcal{A}} = \int \frac{d^3k'}{(2\pi)^3}(\vec{\rho} - \vec{\bar{\rho}})$$

$$\frac{d\vec{\mathcal{A}}}{dt} = \mathcal{F} y_{\rm eff} \left[\vec{\mathcal{H}}_0(y_{\rm eff}) + \vec{V}_c(y_{\rm eff})\right] \times \vec{\mathcal{A}}$$

Adiabatic MSW transition

- If the frequency of synchronous oscillations is fast compared to the MSW transition time scale, the asymmetry vector will follow smoothly (adiabatically) the MSW transition of the Hamiltonian:

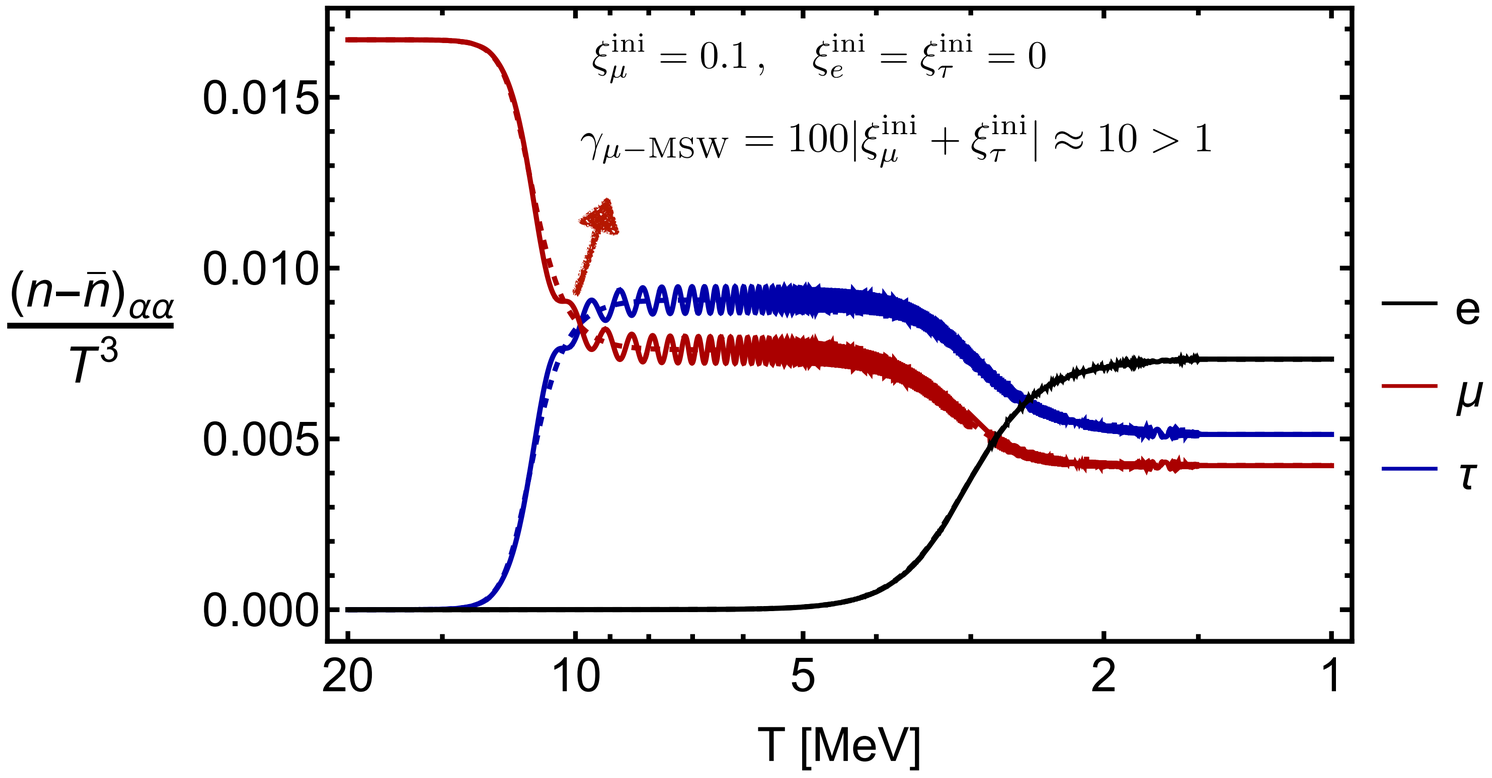

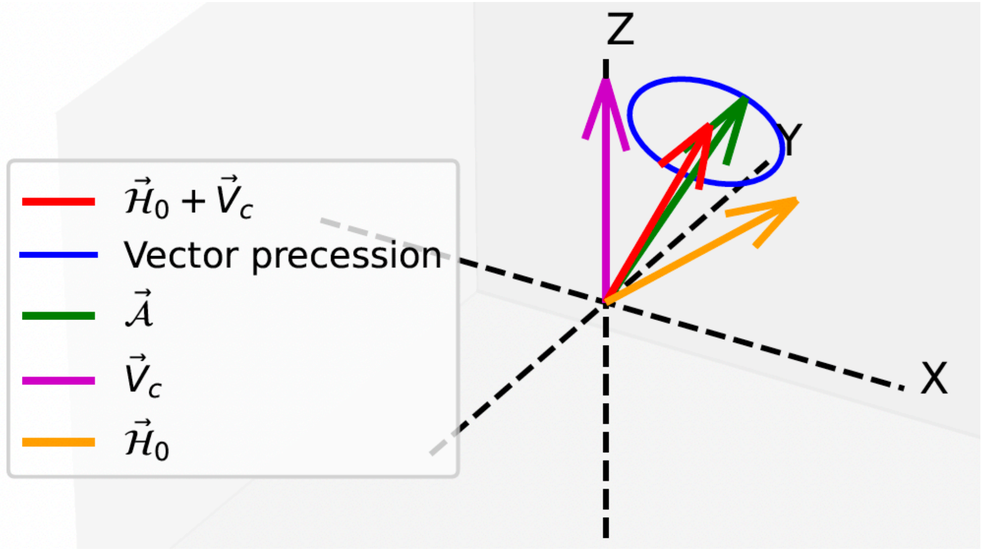

- The self-interactions fully dominate such that $[V_s, r(\bar{r})] \approx 0$, we can set $V_s = 0$ to average the fast oscillations (dashed lines)

Non-adiabatic MSW transition

- If the frequency of synchronous oscillations is slow compared to the MSW transition time scale, the asymmetry vector will be unable to follow smoothly the MSW transition of the Hamiltonian.

$$\xi_\mu^{\rm ini} = -\xi_\tau^{\rm ini} = 0.92\,, \quad \xi_e^{\rm ini} = 0$$

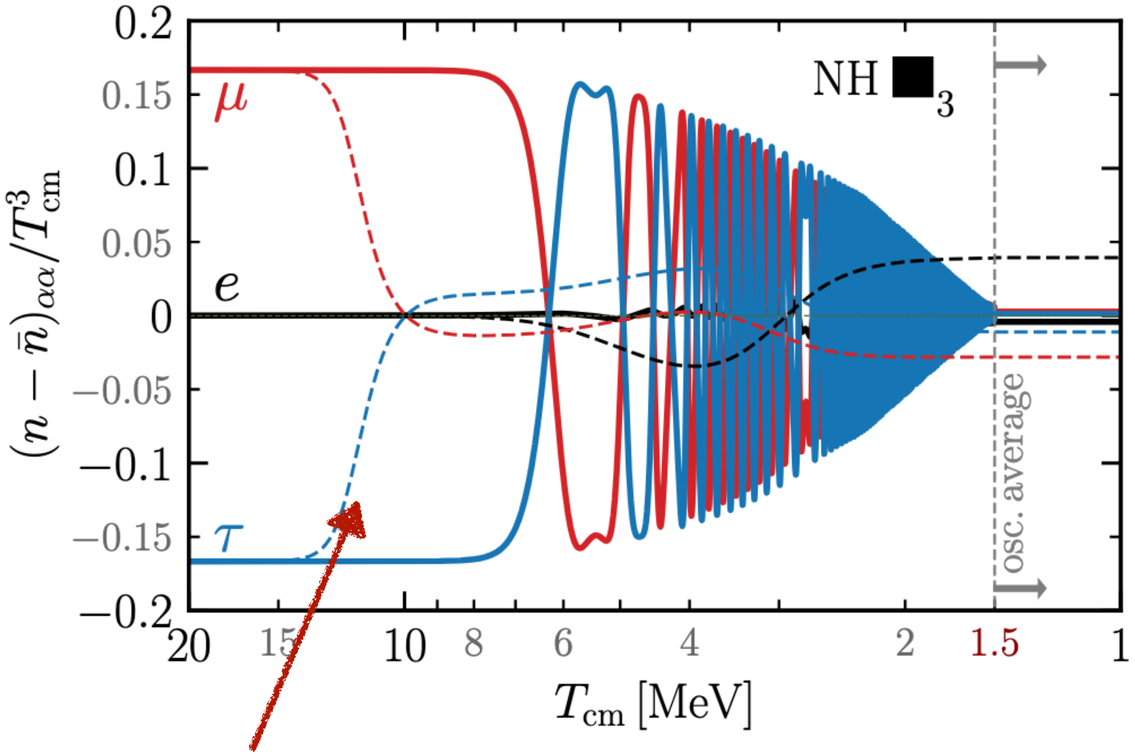

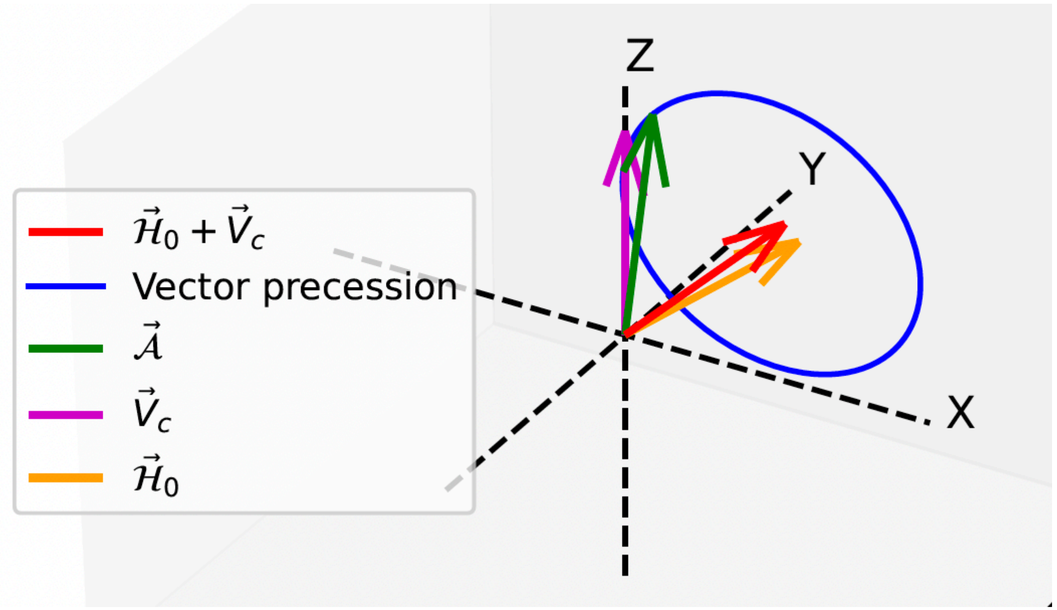

$$\gamma_{\mu-\rm MSW} = 100|\xi_\mu^{\rm ini} + \xi_\tau^{\rm ini}| \approx 0 \ll 1$$

Non-adiabatic behaviour leads to delayed MSW transition

Backup: actual equations

$$
\begin{aligned}
&Hxr' + 3Hxr\frac{z_\nu'}{z_\nu} = \\
&\quad - i\left[\frac{\pi^2}{36\zeta(3)}UM^2U^\dagger\frac{1}{z_\nu}\left(\frac{x}{T_{\rm ref}}\right) - 2\sqrt{2}\frac{7\pi^4}{180\zeta(3)}\frac{G_F}{m_W^2}z_\nu z_\gamma^4\left(\frac{T_{\rm ref}}{x}\right)^5(\mathbb{E}+\mathbb{P}) - \frac{3\zeta(3)G_F}{2\pi^2\sqrt{2}}z_\nu^3\left(\frac{T_{\rm ref}}{x}\right)^3\bar{r}, r\right] + \langle\mathcal{I}\rangle\,, \\
&Hx\bar{r}' + 3Hx\bar{r}\frac{z_\nu'}{z_\nu} = \\
&\quad + i\left[\frac{\pi^2}{36\zeta(3)}UM^2U^\dagger\frac{1}{z_\nu}\left(\frac{x}{T_{\rm ref}}\right) - 2\sqrt{2}\frac{7\pi^4}{180\zeta(3)}\frac{G_F}{m_W^2}z_\nu z_\gamma^4\left(\frac{T_{\rm ref}}{x}\right)^5(\mathbb{E}+\mathbb{P}) - \frac{3\zeta(3)G_F}{2\pi^2\sqrt{2}}z_\nu^3\left(\frac{T_{\rm ref}}{x}\right)^3 r, \bar{r}\right] + \langle\bar{\mathcal{I}}\rangle\,.
\end{aligned}
\tag{17}
$$

and

$$
z_\nu' = -\frac{z_\nu}{4}\left[\frac{\mathrm{Tr}[r'+\bar{r}']}{\mathrm{Tr}[r+\bar{r}]} - \frac{\frac{1}{H}\frac{\delta\varepsilon}{\delta t}}{x\varepsilon_\nu}\right], \quad z_\gamma' = \frac{z_\gamma}{x} - \frac{4\varepsilon_\gamma + 3(\varepsilon_e + p_e) - \frac{1}{H}\frac{\delta\varepsilon}{\delta t}}{T_{\rm ref}\frac{\partial}{\partial T_\gamma}(\varepsilon_\gamma + \varepsilon_e)}\,. \tag{18}
$$

$$
x = T_{\rm ref}/T_{\rm cm}\,, \quad y = k/T_{\rm cm}\,,
$$

$$
z_\gamma = T_\gamma/T_{\rm cm}\,, \quad z_\nu = T_\nu/T_{\rm cm}\,.
$$

$$
\begin{aligned}
r^{0\prime} &= c^0\,, \quad r^{i\prime} = 2f^{ijk}r^k\left(h_0^j + v_c^j - v_s\bar{r}^j\right) + c^i\,, \\
\bar{r}^{0\prime} &= \bar{c}^0\,, \quad \bar{r}^{i\prime} = -2f^{ijk}\bar{r}^k\left(h_0^j + v_c^j - v_s r^j\right) + \bar{c}^i\,.
\end{aligned}
$$

Backup: Collisions

- In our momentum average ansatz, collisions can be casted in analytical form in the limit $m_e \to 0$

$$\langle \mathcal{I}_{12\leftrightarrow 34}\rangle = \frac{1}{\int \frac{\mathrm{d}^3\vec{k}_1}{(2\pi)^3} f_1} \int \frac{\mathrm{d}^3\vec{k}_1}{(2\pi)^3 2E_1} \frac{\mathrm{d}^3\vec{k}_2}{(2\pi)^3 2E_2} \frac{\mathrm{d}^3\vec{k}_3}{(2\pi)^3 2E_3} \frac{\mathrm{d}^3\vec{k}_4}{(2\pi)^3 2E_4} (2\pi)^4 \delta^4(p_1 + p_2 - p_3 - p_4) \times S|M|^2 \times F(f_1, f_2, f_3, f_4)\,. \tag{B3}$$

$$\langle \mathcal{I}\rangle^{\nu e\leftrightarrow \nu e} = 4F_{\rm FD} \frac{8G_F^2 T^5}{\pi^3} z_\gamma^4 z_\nu (1-\epsilon) \left\{ [G^L r G^L (\mathbb{1} - \epsilon\, r) + (\mathbb{1} - \epsilon\, r) G^L r G^L] - [r G^L (\mathbb{1} - \epsilon\, r) G^L + G^L (\mathbb{1} - \epsilon\, r) G^L r] \right\} \tag{C5}$$

$$\begin{aligned} \langle \mathcal{I}\rangle^{\nu\bar{\nu}\leftrightarrow e^+e^-} &= F_{\rm FD} \frac{8G_F^2 T^5}{\pi^3} \frac{1}{z_\nu^3} \left\{ z_\gamma^8 [G^L (\mathbb{1} - \epsilon\, \bar{r}) G^L (\mathbb{1} - \epsilon\, r) + (\mathbb{1} - \epsilon\, r) G^L (\mathbb{1} - \epsilon\, \bar{r}) G^L] - z_\nu^8 (1-\epsilon)^2 [r G^L \bar{r} G^L + G^L \bar{r} G^L r] \right\} \\ &+ F_{\rm FD} \frac{8G_F^2 T^5}{\pi^3} \frac{1}{z_\nu^3} \left\{ z_\gamma^8 [G^R (\mathbb{1} - \epsilon\, \bar{r}) G^R (\mathbb{1} - \epsilon\, r) + (\mathbb{1} - \epsilon\, r) G^R (\mathbb{1} - \epsilon\, \bar{r}) G^R] - z_\nu^8 (1-\epsilon)^2 [r G^R \bar{r} G^R + G^R \bar{r} G^R r] \right\} \end{aligned} \tag{C6}$$

$$\langle \mathcal{I}\rangle^{\nu\bar{\nu}\leftrightarrow \nu\bar{\nu}} = \frac{1}{4} F_{\rm FD} \frac{8G_F^2 T^5}{\pi^3} z_\nu^5 \left\{ 2\mathrm{Tr}[r\bar{r}][\mathbb{1} - \epsilon\,(r + \bar{r})] - (r\bar{r} + \bar{r}r)(\mathrm{Tr}[\mathbb{1}] - \epsilon\,\mathrm{Tr}[r + \bar{r}]) \right\}, \tag{C7}$$

where as in the main text $T = T_{\rm cm}$, $z_\gamma \equiv T_\gamma / T_{\rm cm}$ and $z_\nu \equiv T_\nu / T_{\rm cm}$. In the limit $F_{\rm FD} \to 1$ and $\epsilon \to 0$, we recover the MB limit outlined in the main text in Eqs. (22), (23), and (24), respectively.

$$G^L = \mathrm{diag}(g_L, g_L - 1, g_L - 1) \qquad G^R = \mathrm{diag}(g_R, g_R, g_R) \qquad g_L = s_W^2 + 1/2 \text{ and } g_R = s_W^2$$

Backup: Initial conditions

- Due to our ansatz for density matrices, any initial conditions is necessarily an approximation to the real system. We choose (to preserve the delicate dynamics of non-daiabatic MSW):

$$r_{\alpha\alpha} = \frac{\int y^2 dy f_{\rm FD}(y,\xi_\alpha)}{\int y^2 dy f_{\rm FD}(y,0)} = \frac{-2{\rm Li}_3(-e^{\xi_\alpha})}{\frac{3\zeta(3)}{2}}\,,$$

$$\bar{r}_{\alpha\alpha} = \frac{\int y^2 dy f_{\rm FD}(y,-\xi_\alpha)}{\int y^2 dy f_{\rm FD}(y,0)} = \frac{-2{\rm Li}_3(-e^{-\xi_\alpha})}{\frac{3\zeta(3)}{2}}\,.$$

- Take into account $T_\nu \neq T_{\rm cm}$ and enforce detailed balance (thermal and chemical eq.)

$$r^{\rm ini}_{\alpha\alpha} = -\frac{4z_\nu^{-3}}{3\zeta(3)}{\rm Li}_3\left(-{\rm e}^{\xi_\alpha}\right) + \epsilon^\alpha_{\rm db}\,, \quad \bar{r}^{\rm ini}_{\alpha\alpha} = -\frac{4z_\nu^{-3}}{3\zeta(3)}{\rm Li}_3\left(-{\rm e}^{-\xi_\alpha}\right) + \epsilon^\alpha_{\rm db} \quad ({\rm initial\,conditions})\,. \tag{31}$$

Backup: Comparison with momentum-dependent

- Dataset of about 2300 points computed with full momentum-dependent code by Froustey and Pitrou [2405.06509]:

$$\delta n_\alpha \equiv \max\left[\left|\frac{(n-\bar{n})^{\text{this work}}_{\alpha\alpha}}{(n-\bar{n})^{\text{Froustey+}}_{\alpha\alpha}}\right|, \left|\frac{(n-\bar{n})^{\text{Froustey+}}_{\alpha\alpha}}{(n-\bar{n})^{\text{this work}}_{\alpha\alpha}}\right|\right] - 1\Bigg|_{\text{BBN}},$$

- 85% of points → $\delta n_\alpha \leq 1$ out of this 47%(11%) → $\delta n_\alpha \leq 0.1(0.01)$

- Focusing on the remaining 15% which show poor agreement, 83% are excluded, and 43% fall in particular flavour directions:

$$\Delta n_\tau = \Delta n_\mu \simeq -\Delta n_\mu / c \qquad\qquad c = 2,\ 1.83$$

The (flavour) asymmetric Universe

- Matter asymmetry in the early Universe is related to a difference between the number densities of matter and anti-matter.

- In the case of thermal equilibrium, the asymmetry is parameterised in the form of a chemical potential μ:

$$f_{\mathrm{FD}} = \frac{1}{e^{\frac{E \mp \mu}{T}} + 1}$$

$$\xi \equiv \frac{\mu}{T}$$

→ Comoving chemical potential

$$n = g \int \frac{d^3k}{(2\pi)^3} f(k,T)$$

$$\Delta n = \frac{n - \bar{n}}{T^3} = \frac{1}{6}\left(\xi + \frac{\xi^3}{\pi^2}\right)$$

Comoving asymmetry

for FD distribution